공학석사학위논문

Regenerable Antifouling Reverse Osmosis Membrane with Electro-Responsive Hydrophilic Complex

전기감응성 친수성 복합체로 개질된
재생 가능한 내오염성 역삼투 분리막에 대한 연구

2018년 2월

서울대학교 대학원
재료공학부
이 지 영

Abstract

Regenerable Antifouling Reverse Osmosis Membrane with Electro-Responsive Hydrophilic Complex

Jiyoung Lee
Department of Materials Science and Engineering
The Graduate School
Seoul National University

We developed electro-responsive thin film composite polyamide reverse osmosis (RO) membrane with regeneration property and anti-fouling property by introduction hydrophilic modified ferrocene (Fc)-cyclodextrin (CD) complex. Modified RO membrane can be regenerated by attaching and detaching the cyclodextrin with electrical treatment. First, we prepared branched Polyethylenimine modified with ferrocene (b-Fc). Various composition of b-Fc was synthesized to optimize the performance. A commercial thin film composite polyamide RO membrane was improved

with b-Fc using carboxyl group function by carbodiimide-induced grafting. Then, Cyclodextrin and ferrocene were combined with the introduction of cyclodextrin. Successful synthesis of b-Fc was observed by Fourier transform infrared spectroscopy (FT-IR) and proton nuclear magnetic resonance (^{1}H NMR). Furthermore, successful preparation of electro-responsive hydrophilic complex-modified RO membrane was confirmed by attenuated total reflectance Fourier transform infrared (ATR FT-IR) and X-ray spectroscopy (XPS) analysis. Also, Field emission scanning electron microscopy (FE-SEM), atomic force microscope (AFM), and water contact angle measurement were additionally implemented to define the surface property of the membrane surface. Finally, filtration tests were conducted to evaluate the water flux, NaCl rejection, anti-fouling property, and recovery performance. As expected, the modified membrane showed high antifouling property and the water flux of modified membrane could be recovered to 86.4% after electrical treatment. Therefore, we demonstrated that regenerable membrane exhibiting high recovery from fouling was successfully developed.

Keywords

Reverse osmosis membrane, Fouling, Electro-responsive, branched-Polyethylenimine (b-PEI), Regenerable,

Student number: 2016-20816

Contents

1. Introduction

In recent years, water shortage is the foremost global risk to social, environment around the world. It is exacerbated by water pollution, rapid growth in the world's population, and global climate change [1]. Thus, the demand for fresh water has dramatically accelerated efforts toward development of water reuse and seawater desalination [2]. The two most successful commercial water desalination techniques are thermal and membrane systems.

Membrane technology is one of the most promising ways to produce fresh water [3, 4]. The common membrane technologies for water desalination is reverse osmosis (RO) [5]. It is currently the most energy-efficient technology and has low capital and operating costs compared with thermal process. Also, RO membrane has the high water permeability and salt rejection. The current RO membrane market is dominated by thin film composite (TFC) polyamide (PA) membranes [6, 7]. The functional layer was prepared by the interfacial polymerization of m-pheylenediamine (MPD) in the water and trimesoyl chloride (TMC) in hexane on the polysulfone support layer. The support layer provides the required mechanical stability under high pressures and the polyamide layer plays the principal role in water filtration.

However, a critical drawback in reliable RO membrane performance is fouling. Fouling is mainly caused by the multi-interactions between the membrane surface and the pollutants, like electrostatic and hydrophobic interactions. Formation of a fouling layer on the membrane surface leads to decline in permeate flux and quality, and reduce the membrane life time. All these factors make the increase of operating cost [8]. In order to control the membrane fouling, a variety methods have been studied. One of the typical solution is surface modification to alter the hydrophilicity or charge properties so as to improve the fouling resistance of the membranes [9, 10, 11]. The fouling resistance of the membrane could be enhanced without significantly affecting other properties. However, these fouling resistant membranes will not endure after formation of the first fouling layer on the membrane surface and eventually membrane replacement is required. Therefore, it is necessary to develop a new approach to recover the anti-fouling property of a membrane from accumulated foulants.

A promising candidate membrane material for such ultimate fouling control is stimuli-responsive material. Stimuli-responsive materials are capable of conformational and chemical changes on receiving an external stimulus [12]. Through this property, stimuli-responsive membranes can change their properties in response to external signals [13]. The membrane responsive to temperature [14, 15], pH [16, 17], electrolytes [18], magnetism

[19], and electric fields [20] have been developed. The stimuli-responsive membranes can change the surface property by applied stimulus, providing a driving force to enable the release of the foulants. These membranes show good anti-fouling property but still require higher recovery from fouling. As a result, stimuli-responsive characteristics have recently been studied for improving the fouling control of membrane by releasing of the severely fouled membrane active layer and regeneration of a fresh one.

S. Y. Park et al. [21] introduced a hydrophilic layer on to the membrane surface with a covalently thermo-reversible diels-alder cycloaddition for regenerable membrane. The hydrophilic layer is detached after contamination and attached with new layer on the surface of PTFE membrane by adjusting temperature, and the resulting membrane displayed excellent anti-fouling properties. P. Ahmadiannamini et al. [22] introduced sacrificial polyelectrolyte multilayer with layer-by-layer method. A fouled membrane was soaked in a buffer solution at pH 10 and polyelectrolyte active layer, such as poly (acrylic acid), can disassemble from the membrane surface as a sacrificial layer along with the irreversible foulants. Membrane can be regenerated by re-deposition polyelectrolyte multilayer and showed nearly complete recovery of water flux and rejection after irreversible fouling. The similar method using polyelectrolyte multilayer was investigated on forward osmosis process [23]. By using Polyethylenimine

and poly (acrylic acid) as multilayers, membrane has regeneration property for fouling control by removing the polyelectrolyte active layer at acid condition and assembling in situ a new polyelectrolyte layer.

Compared to other stimulus, electric field can be easily and quickly applied to membrane in a large area without damage the membrane, so it is the most suitable stimulus for membrane application. β-cyclodextrin (β–CD) and Ferrocene (Fc) complex also can be used as electro-responsive material for regenerable membrane [24]. β–CD is with 7 glucoside units, and can interact with many guests with suitable sizes forming supramolecular [25, 26, 27]. The typical example of complex pairs is β–CD and Fc. β–CD can form a stable inclusion complex with Fc with a formation constant of 2200 M^{-1} and this complex can be reversibly associated and dissociated by charging the Fc species with electric field [28, 29]. T.-W. Chou et al. [24] utilized electro-responsive Fc/CD complex for membrane cleaning. They detached the protein by changing property of surface using electro-responsive complex as reversible cross-linker of grafting polymer on PTFE membrane. Dissociation of the cross-linked complex with an electric-field provides high recovery performance and membrane can be reworkable by recrosslinking the modified layer. Nevertheless, this method can aggravate the fouling due to low hydrophilic grafting polymer and also can decrease water flux severely by blocking the pores by multi-layers of cross-linker. In conclusion, new

effective method to introduce Fc/CD is required which is not applicable to multi-layer structure and also has antifouling property with recovery performance.

Here, we prepared electro-responsive hydrophilic complex using branched Polyethylenimine (b-PEI) modified with Fc/CD complexes. b-PEI has lots of amine groups that can endow hydrophilic nature and be easily converted to reactive functional group [30, 31]. Amine groups give high anti-fouling property by hydrophilicity and help oxidation of ferrocene by weak polyelectrolyte property [32]. Also, high density of amine groups introduce the functional groups efficiently without multilayer structure and can control the amounts for high recovery performance. So, electro-responsive regeneration effect can be applied with antifouling property and performance maintenance using b-PEI with Fc/CD complex.

Based on the above analysis, TFC PA RO membrane surface modified with electro-responsive hydrophilic complex have been prepared. The electro-responsive hydrophilic complex are grafted by chemical method on the conventional TFC PA RO membrane. Then, surface characteristics of membrane were confirmed through SEM, XPS, AFM and contact angle. Finally, permselectivity and fouling test were investigated. The performance and fouling resistance of modified and unmodified membranes were also compared. As expected, the resulting membrane had antifouling property by

hydrophilicity of membrane surface and regeneration property by attaching and detaching the cyclodextrin with electrical treatment. The novel and efficient approach to regenerable TFC PA RO membrane from fouling has been demonstrated.

2. Experimental

2.1. Materials

A commercially available aromatic polyamide RO membrane (RE2521-TL, Woongjin Chemical Co., Ltd., Korea), which was fabricated by interfacial polymerization using TMC and MPD on polysulfone support, was used as the base matric for grafting. 1-Ethyl-3(3-dimethyl amidopropyl) carbodiimine (EDC, 98.5%), N-hydroxysuccinimide (NHS, 98%), Polyethylenimine (b-PEI, branched, M_w=25,000), Ferrocenecarboxaldehyde (FcCHO, 98%), β-cyclodextrin (β-CD), and Cetyltrimethylammonium chloride solution (CTAC) were purchased from Sigma-Aldrich (St Louis MO, USA). Sodium borohydride ($NaBH_4$, 0.99) was purchased from Fluka. Sodium hypochlorite solution (NaOCl, 10 wt% free chlorine) used in membrane cleaning solution and Methanol (99.5%) were purchased form Daejung Chemical & Metals (Gyeonggido, Korea). Diethyl eter (99.0%) was purchased from Samchun Chemical. Aqueous solutions were prepared with deionized (DI) water.

2.2. Synthesis of ferrocene-modified branched Polyethylenimine (b-Fc)

Synthesis of b-Fc was conducted similarly as procedures in previously reported method [32]. B-PEI (1.75 g) was dissolved in 60 ml of methanol in a round-bottom flask. After that, a solution of 0.7484 g (3.5 mmol) of ferrocenecarboxaldehyde dissolved in 6.0 ml of methanol was added to it drop-wise under constant agitation. The resulting dark red solution was stirred for 2 h with magnetic stirrer and cooled in an ice bath. Sodium borohydride (0.1326 g, 3.5 mmol) was slowly added by dropping pipette, during which time the solution lightened in color. The mixture was stirred continuously for 1 h. After then, residues were filtered with cellulose filter paper (Advantac, average pore size 0.45 μm). The methanol in the mixture was removed by a rotary evaporator and dried in a vacuum drier for 12 h. The raw product was extracted with diethyl ether for 24 h and dried under vacuum overnight. Overall scheme is subscribed in **Figure 1.**

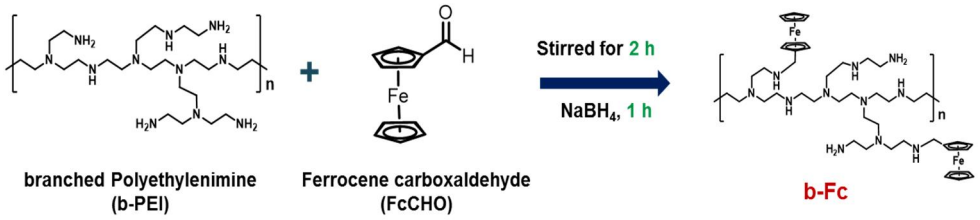

Figure 1. Schematic illustration of synthesis of b-Fc.

2.3. Fabrication of b-Fc/CD-modified RO membrane

The primary modification involved a two-stage activation process, and the schematic diagram of the modification process was shown in **Figure 2**. b-Fc was grafted to the aromatic polyamide RO membrane surface through amide bond by the carbodiimide-induced method. The EDC was used as the activating agent while NHS was used as the stabilizer. 60 mg of EDC was dissolved in 60 ml of deionized water to prepare 0.1 wt. % EDC solution in 70 ml vial. The thoroughly washed RO membrane (6 cm × 5cm) was immersed in the EDC solution at 4 °C for 15 min. EDC first reacted with the carboxyl group on the membrane surface and formed an unstable reactive 0-acylisourea ester intermediate. And then, 60 mg of NHS was added in to the vial to activate the carboxylic acid groups on the membrane surface. The NHS reacted with the O-acylisourea ester to form the semi-stable amine-reactive NHS-ester intermediate. Both of the unstable reactive O-acylisourea ester and the semi-stable amine reactive NHS-ester intermediate could react with the amine group of b-Fc. The membrane was gently washed twice with deionized water and then incubated in a 1g/L b-Fc aqueous solution. Membrane was sealed and placed in a dark place at room temperature for 24 h. The resulting membrane was thoroughly washed and stored in pure water. This membrane referred to as RO/b-Fc.

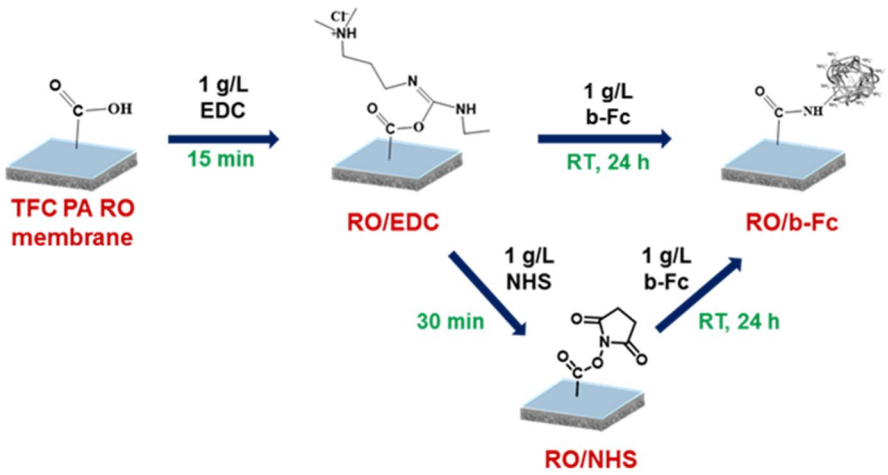

Figure 2. Schematic illustration of fabrication of RO/b-Fc

RO/b-Fc membranes were immersed in an aqueous solution of β-cyclodextrin (1 $mgmL^{-1}$). The membrane was kept in the solution at room temperature for 24h. Then, the membranes were draw out, washed with deionized water. The obtained samples were coded as RO/b-Fc/CD and illustrated at **Figure 3.**

2.4. Electrical treatment process

The cyclodextrin can be freely detached and re-attached by electrical treatment. As previously described, the association and dissociation reaction between β-CD and ferrocene is reversible. The dissociation reaction occurred by oxidation of ferrocene to ferrocenium under electrical treatment. To remove the CDs from the surface, membranes were attached on the anode. Metal plates (aluminum, copper, titanium) and carbon plates were used as electrodes. Electrodes were immersed in a NaCl solution (0.5 M), which was similar concentration with seawater. An electrical field was applied for 30 s. At this potential water oxidation occurred, and resulted the formation of Fc^+ along the anode.

$$2Fc \rightarrow 2e^- + 2Fc^+$$

$$2Cl^- \rightarrow Cl_2 + 2e^-$$

The corresponding half reaction took place on the cathode

$$4H_2O + 4e^- \rightarrow 4OH^- + 2H_2$$

After then, electrical treatment the membranes were washed with deionized water to remove loosely attached CDs. This membrane referred to as RO/b-Fc*. Overall scheme is subscribed in **Figure 4.**

The re-attachment of CDs occurred with similar method. RO/b-Fc* membranes were attached on the cathode to reduction the ferrocenium. Electrodes were immersed in a NaCl solution (0.5 M) and applied electric field for 30 s. The following equations showed the reaction on cathode.

$$2e^- + 2Fc^+ \rightarrow 2Fc$$

$$2H_2O + 2e^- \rightarrow 2OH^- + H_2$$

After electrical treatment, membranes were soaked in deionized water overnight. The washed membrane were immersed in an aqueous solution of β-cyclodextrin (1 $mgmL^{-1}$) kept with an ultrasonic bath at room temperature for 1 h. After 24 h, the membranes were draw out and washed with deionized water. The obtained membranes were coded as R-RO/b-Fc/CD. Carbon plates and metal plates were purchased form the market. An electric field was applied to the solution using a 9V dry cell (Panasonic Inc.).

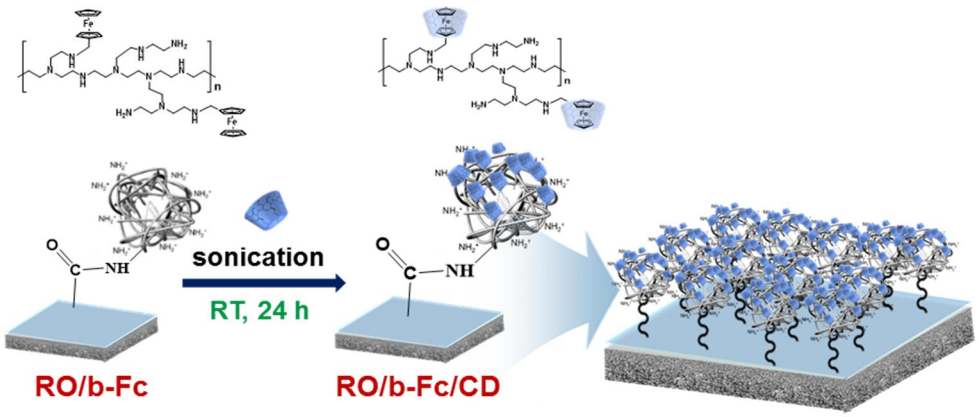

Figure 3. Schematic illustration of fabrication of RO/b-Fc/CD

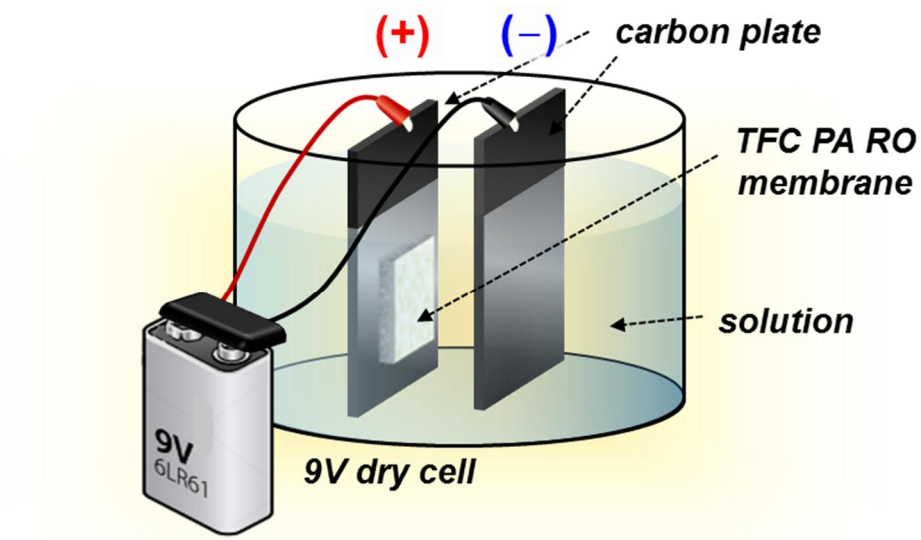

Figure 4. Schematic illustration of electrical treatment process

2.5. Characterization

2.5.1. Characterization of b-Fc

Chemical structure of synthesized b-Fc was monitored by Fourier transform infrared (FT-IR, Thermo Scientific Nicolet iS1) spectroscopy. FT-IR spectra was collected on samples palletized with KBr powders over the range of 500-4000 cm^{-} with a spectral resolution of 4 cm^{-1}. The proton nuclear magnetic resonance (^{1}H NMR, Bruker AVANCE 600) spectroscopy in $CDCl_3$ was performed to calculate substation degree by comparing integral ratio of Fc and b-PEI. In order to compare the size of b-Fc, 0.5 mg/mL concentration of b-Fc was dissolved in deionized water, and then analyzed by Dynamic light scattering (DLS, DLS-7000) spectrophotometer.

2.5.2. Characterization of membrane

TFC PA RO, RO/b-Fc, RO/b-Fc/CD, RO/b-Fc*, and R-RO/b-Fc/CD membranes were characterized by attenuated total reflection Fourier transform infrared (ATR FT-IR, Thermo Scientific Nicolet iS5) spectroscopy with a spectral resolution of 4 cm-1 with the range of 650-4000 cm-1. Spectra were recorded in air in the ATR mode using a zinc selenite tip mode. The elemental analysis of membranes were characterized by X-ray photoelectron spectroscopy (XPS, Thermo VG Scientific, Esat Grinstead,

UK) at a background pressure of about 1.0×10^{-9} Torr. The instrument employed a monochromated Al Kα X-ray source (hν = 1486.6 eV) which was used at 300 W (15 kV × 20 mA). The area of analysis was approximately 15 μm diameter for the interface sample. The pass energy was set at 20 eV for high-resolution spectra of all elements of interest. All binding energies were calibrated relative to the C 1s peak at 285 eV.

The surface morphology of membranes were observed by field-emission scanning electron microscope (FE-SEM, Carl Zeiss SUPRA 55VP) with an applied voltage of 3.0 kV. Each sample were dried under vacuum and, prior to FE-SEM analysis, were coated with platinum by a vacuum electric sputter coater. The roughness of membranes were observed by atomic force microscope (AFM, Park Systems NX-10) operated in the tapping mode. Tapered coating samples were fixed to metal AFM stubs prior to analysis.

To evaluate the hydrophilicity of the membrane surface, static pure water contact angle measurement (Biolinscientific, Attention® THETA LITE) was used under room temperature using deionized water.

2.6. Performance evaluation

2.6.1. Permselectivity evaluation

Water flux, rejection, and anti-fouling property of RO/b-Fc/CD were measured by filtration system described in **Figure 5**. The tests were carried out using Sterlitech HP4750 stirred cell connected to a pressure gauge (Millipore Corp.) and the nitrogen gas cylinder. The cell had a teflon-coated magnetic stir bar providing agitation to reduce concentration polarization of cake formation typical of "dead-end". The effective membrane area of membrane area was 14.6 cm^2.

The water flux of RO/b-Fc/CD was evaluated under the conditions below. The reservoir was filled with pure deionized water, and filtration test was performed at 14 bar until the water flux was saturated for 5 min. During the filtration, the weight difference of filtered water was recorded for every 10 seconds by an electronic balance (CUW4200H CAS corp.) that was linked to a computer for automated data gathering at wished time intervals. The flux J_w was calculated as equation (1).

$$\boldsymbol{J_w = \frac{V}{A\Delta t}} \quad (1)$$

J_w is pure water permeability (L/m^2h), V is the volume of filtrated water (L), A is the effective membrane area (m^2), and Δt is permeation time (h).

To evaluate the salt rejection, the NaCl solution (2000 ppm) was prepared as feed solution and then filtrated at 14 bar. After passing the initial filtrate, filtrate was collected in 70 ml vial. The concentration of NaCl was determined by the conductivity of solution using multi meter instrument (CP-500L, ISTE corp.). The salt rejection was calculated as follows:

$$\mathbf{R}(\%) = (\mathbf{1} - \frac{C_p}{C_f}) \times \mathbf{100} \quad (2)$$

Where, C_p and C_f were the salt concentration of permeate solution and feed solutions.

2.6.2. Fouling resistance evaluation

The fouling resistance and the cleaning efficiency of RO/b-Fc/CD were measured by the following filtration systems. The filtration test was performed at 14 bar and cation surfactant (CTAC) was used as foulant. During the filtration, the corresponding water flux was recorded by an electronic balance (CUW4200H CAS corp.). Pure deionized water was permeated for 20 min. Then CTAC solution (60 mg/l) was permeated until the water flux was saturated in order to contaminate the membrane. The fouled membrane was washed by deionized water and soaked overnight. This experiment was repeated three times. After that, the electrical treatment was performed on the membrane to recover from the contamination.

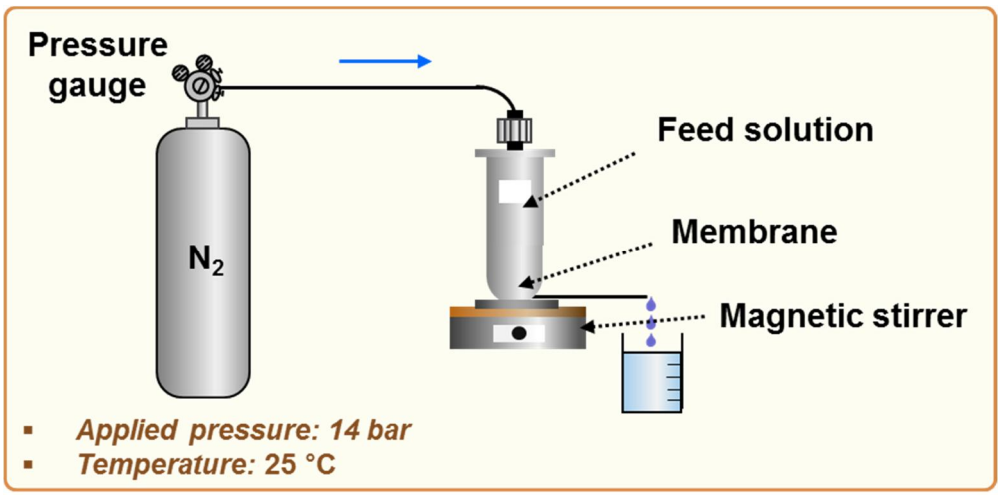

Figure 5. Schematic description of water filtration system

3. Results and discussion

3.1. Synthesis of b-Fc

To find the best recovery efficiency, synthesis of b-Fc was conducted with different ratio of b-PEI and ferrocene. The amount of Fc was set as variable and was shown in **Table 1**. The results of b-Fc were identified with FT-IR and ^{1}H NMR.

Figure 6 showed the chemical structure of pristine b-PEI, FcCHO, and b-Fc by FT-IR spectra. The characteristic peaks of b-Fc are bending vibration of the NH_2 groups at 1640 cm^{-1}, symmetric and asymmetric stretching bands of imine groups at 1045 cm^{-1} and 1105 cm^{-1}. The absorption peaks at 1475, 2838, and 2943 cm^{-1} were observed due to the symmetric and asymmetric stretching bands of sp^3 C-H, respectively. In addition, sp^2 C–H stretch at 3029 cm^{-1} and sp^2 C-H bend at 820 cm^{-1}, which are the peaks of cyclopentadienyl ring in FcCHO, appeared after polymerization and the intensities of peak increased as the composition of ferrocene increased. Especially, C=O stretch at 1679 cm^{-1} disappeared, which verifying that all FcCHO was reacted with b-PEI. To summarize, b-Fc was successfully synthesized with various ratios.

The 1H NMR spectra is represented in **figure 7**. The main peak of b-PEI (peak 4, 5, 6, 7, 8, 9) and FcCHO (peak 3) were still observed in b-Fc spectrum. Also, spectrum of aldehyde in FcCHO at 9.98 ppm (peak 1) disappeared and the new peak appeared at 3.49 ppm (peak 10) which was formed by reaction of b-PEI and FcCHO.

The molar ratio of ferrocene and b-PEI was determined by calculating the integration ratio of amine peak 4-9 in b-PEI and cyclopentadienyl ring peak 3, 3' in FcCHO. **Table 2** showed that the calculated ratios were similar with experimental ratios and indicated that most FcCHO were participated in the reaction.

Sample code	b–PEI	FcCHO
b–Fc1	1.75 g (0.07 mmol)	0.187 g (0.87 mmol, 12.5 eqv.)
b–Fc2		0.374 g (1.75 mmol, 25 eqv.)
b–Fc4		0.748 g (3.5 mmol, 50 eqv.)
b–Fc6		1.122 g (5.25 mmol, 75 eqv.)

Table 1. The amount of b-Fc set as an experimental variable

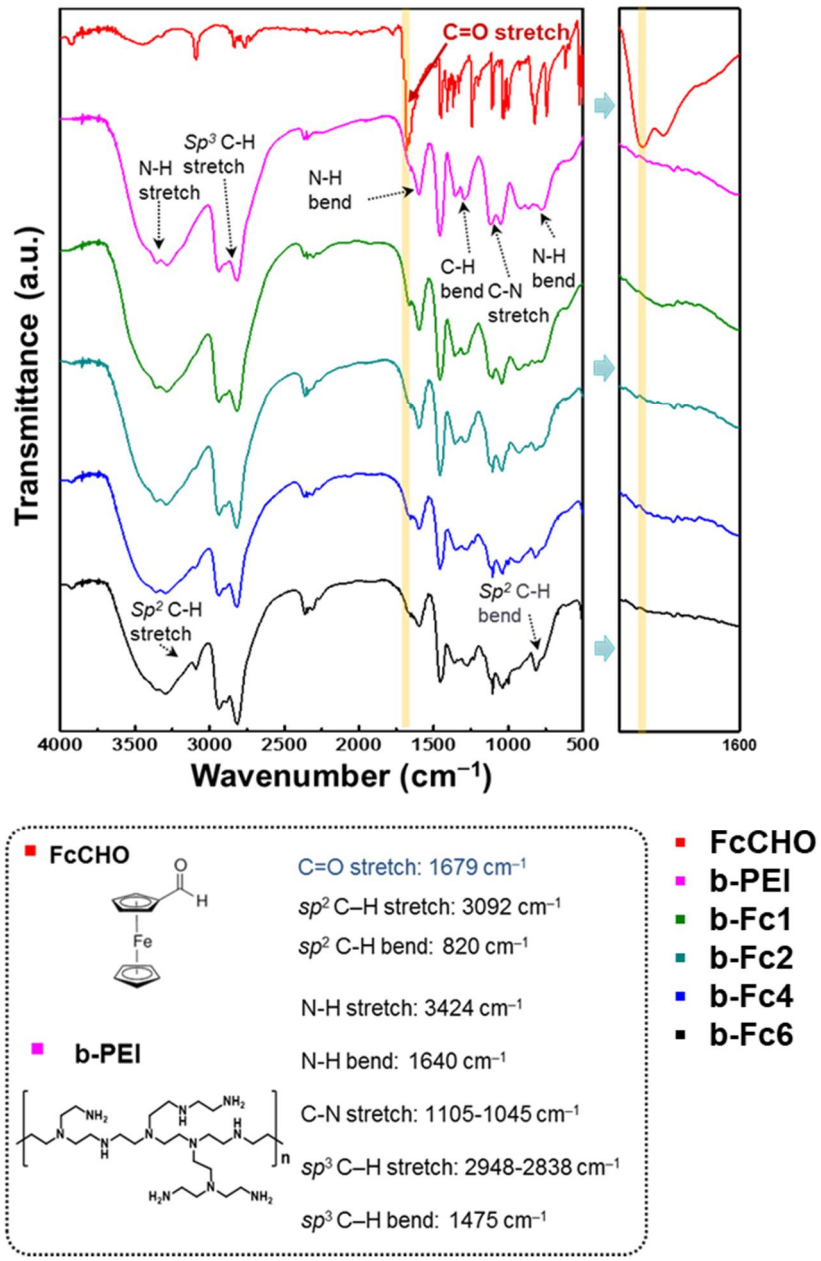

Figure 6. FT-IR spectra of FcCHO, b-PEI, and b-Fc samples

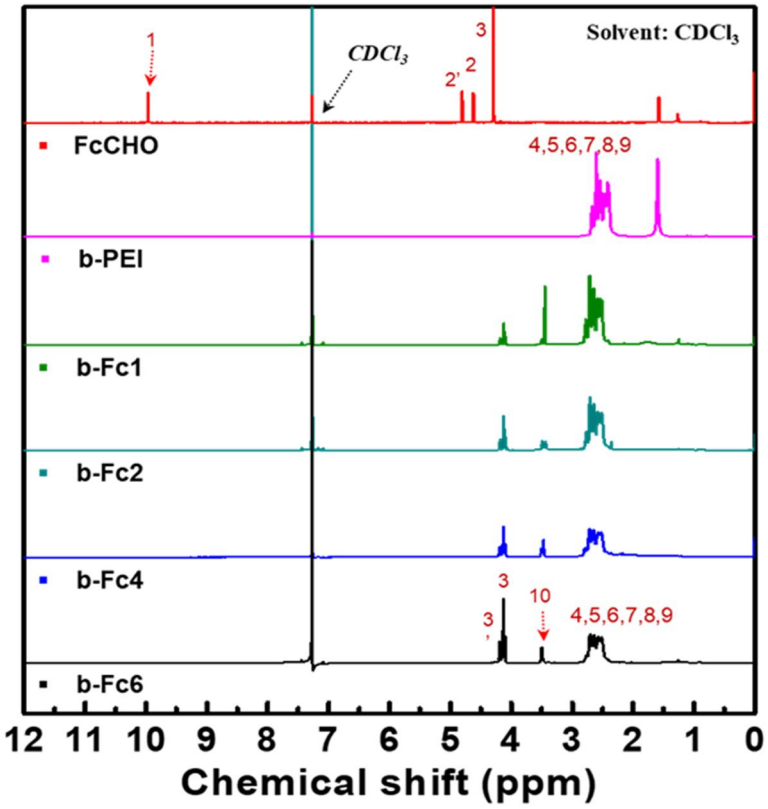
Solvent: CDCl3
CDCl3
1
2'
2
3
FcCHO
4,5,6,7,8,9
b-PEI
b-Fc1
b-Fc2
b-Fc4
3'
3
10
4,5,6,7,8,9
b-Fc6
12 11 10 9 8 7 6 5 4 3 2 1 0
Chemical shift (ppm)

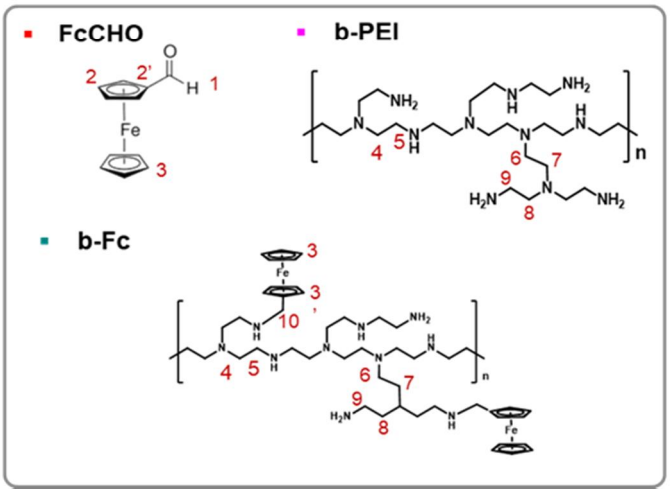
FcCHO
b-PEI
b-Fc

Figure 7. ^{1}H NMR spectra of FcCHO, b-PEI, and b-Fc samples

Sample code	Molar ratio of Fc/b-PEI
b-Fc1	11.0 (12.5 eqv.)
b-Fc2	23.7 (25 eqv.)
b-Fc4	43.9 (50 eqv.)
b-Fc6	71.1 (75 eqv.)

Table 2. Molar ratio of ferrocene and b-PEI calculated by ^{1}H NMR

3.2. Membrane surface characterization

3.2.1. ATR-FTIR analysis

ATR-FTIR spectroscopy provided a convenient and effective way to determine the composition in TFC PA RO membrane. Thus, it is used to verify the successful grafting reaction of NSH, b-Fc, and CD respectively.

Figure 8 and **Figure 9** showed the change of chemical reaction between unmodified and modified membrane. The spectra of TFC PA RO membrane showed characteristic peaks of both polyamide layer (such as N-H bend of amide I at 1660 cm^{-1} and amide II at 1544 cm^{-1}) and polysulfone support membrane (such as S=O stretch of sulfone groups at 1486 cm^{-1} and aromatic ring stretch at 1240 cm^{-1}) because the polyamide layer was thinner than the penetration depth of ATR-FTIR [33]. The additional peak emerged at 1742 cm^{-1} due to C=O stretch of ester group after NHS grafting. RO/b-Fc membranes showed new peak at around 2948-2838 cm^{-1}, which was ascribed to Sp^3 C-H stretch of b-Fc. These results indicated that the b-Fc series were successfully synthesized on to the surface of commercial RO membrane by NHS-induced grafting method.

As shown in **figure 10**, the peak of C-O stretch in glucose ring at 1038 cm^{-1} newly appeared thus confirming the presence of CD. This indicated RO/b-Fc/CD series were successfully synthesized.

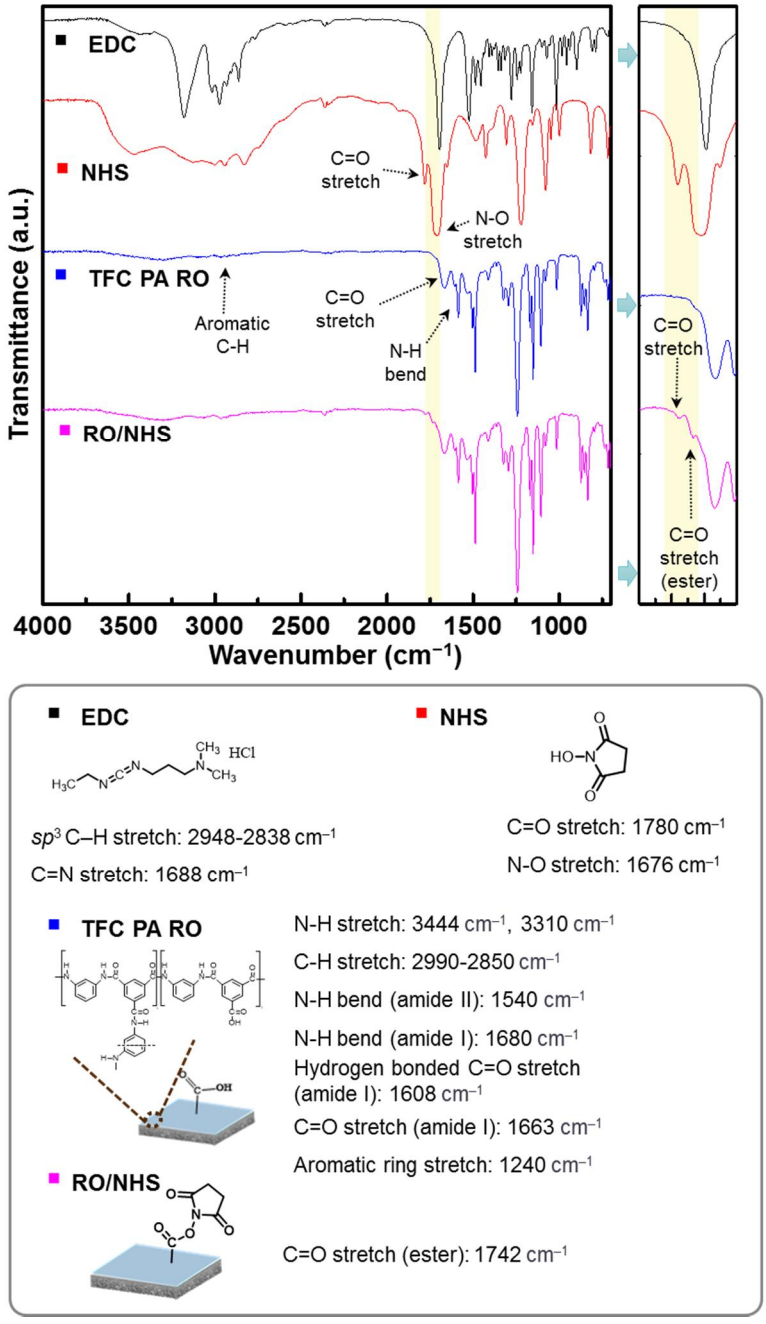

Figure 8. ATR-FTIR spectra of TFC PA RO membrane and RO/NHS

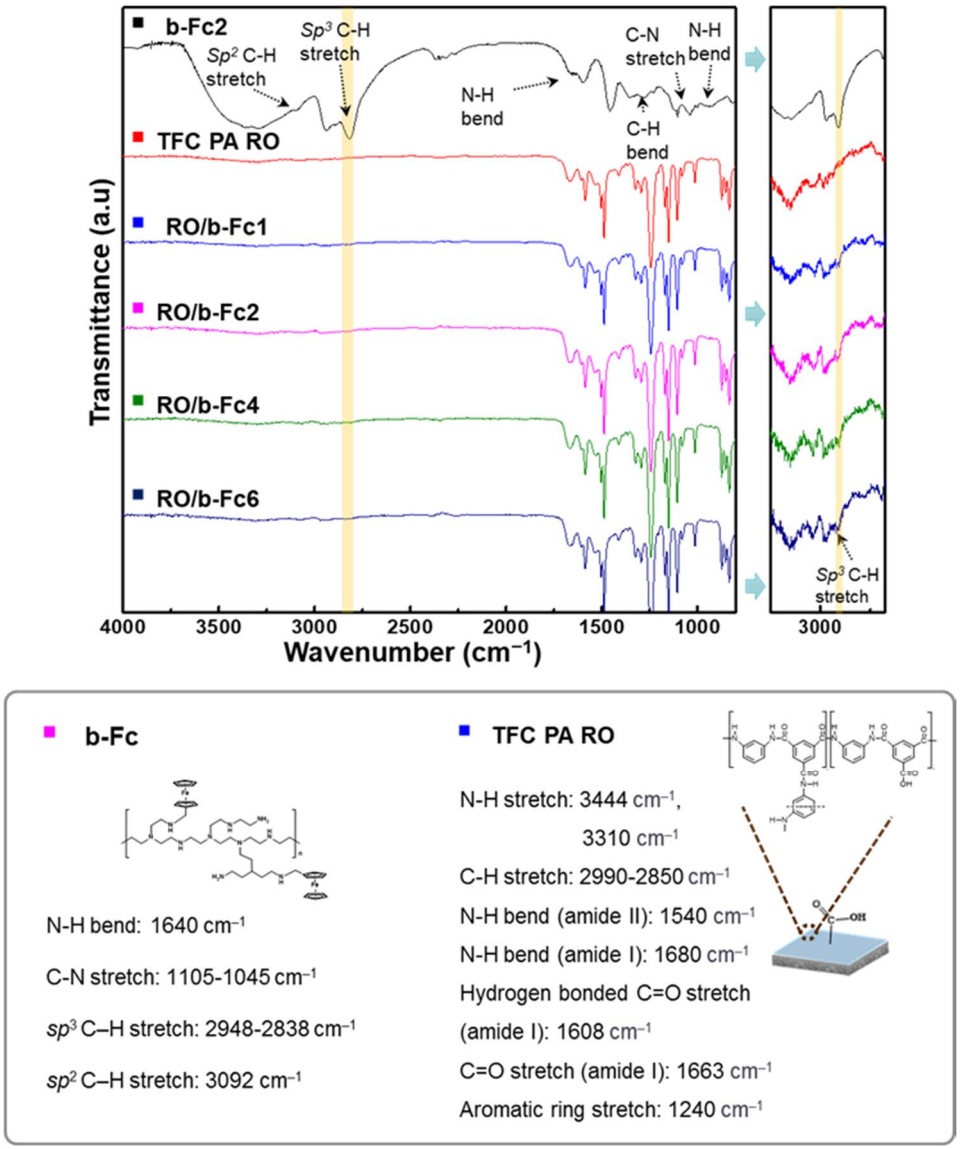

Figure 9. ATR-FTIR spectra of RO/b-Fc membranes

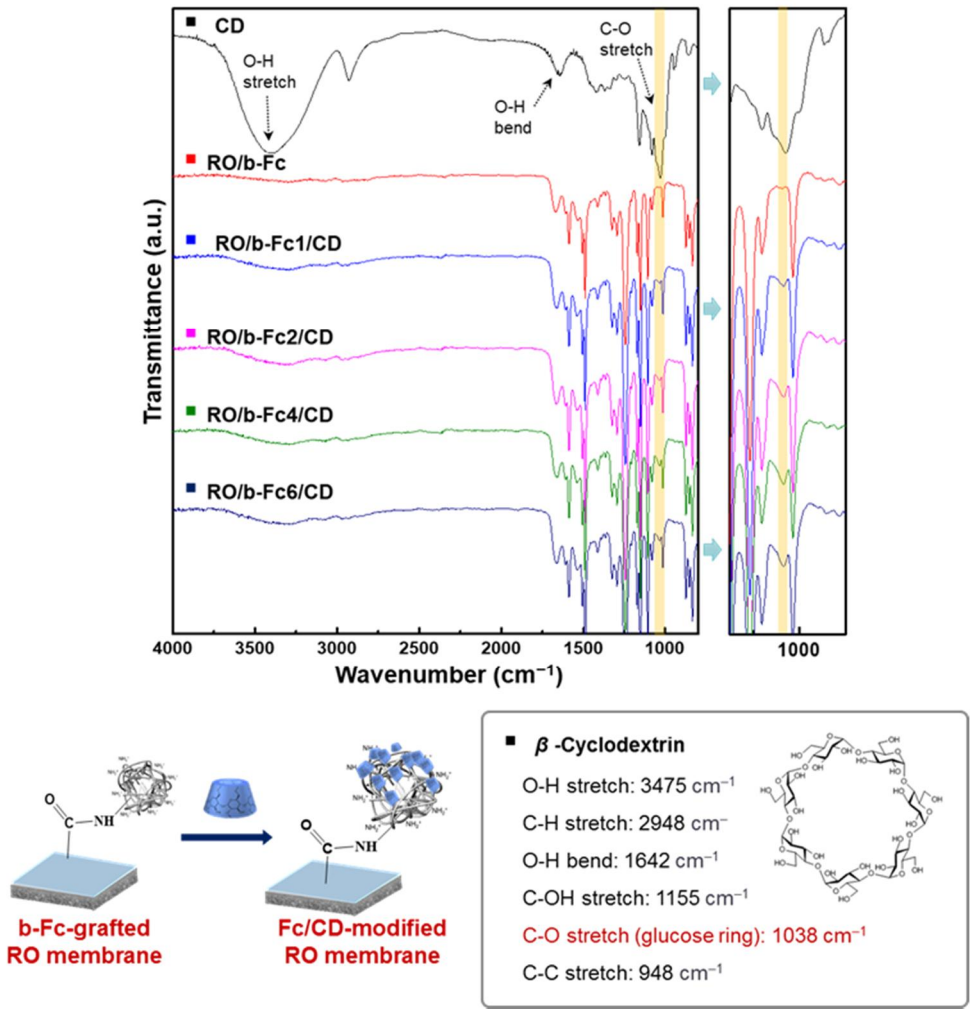

Figure 10. ATR-FTIR spectra of RO/b-Fc/CD membranes

3.2.2. XPS analysis

The effects of the b-Fc and CD modification on the element contents of membrane surface were determined by X-ray photoelectron spectroscopy. The information of chemical bonding was obtained by deconvoluation of C_{1s} and O_{1s} high resolution XPS spectra of the TFC PA RO, RO/b-Fc, and RO/b-Fc/CD as shown in **figure 11.** The C_{1s} high resolution spectra for membranes can be fitted with two main components peak: a major peak at 285 eV for a carbon atom without adjacent electron withdrawing atoms (C-H and C-C species), an intermediated peak at 286.5 eV which is assignable to carbon in weak electron withdrawing (C-N and C-O species) and a minor peak at 288.5 eV which is associated to carbon attached to strong electron withdrawing atoms (C=O) [34]. High resolution O_{1s} spectra had two peaks: C-O at 533.0 eV and C=O at 531.6 eV [35]. The intensity of C-N peak in RO/b-Fc membrane was increased by grafting of b-Fc, because the b-Fc contained higher C-N than the aromatic polyamide top layer of the composite RO membrane. Also, the C-O peak were more distinct in RO/b-Fc/CD. This indicated the successful introduction of the CD on the surface of RO membrane due to the enormous amount of hydroxyl group in CD.

The Fe_{2p} spectrum was showed in **figure 12.** The noise was observed in TFC PA RO membrane. On the other hand, the two peaks at 707.8 eV and 720.4 eV were observed in RO/b-Fc and RO/b-Fc/CD which was associated to binding energy of $2_{p2/3}$ and $2_{p1/2}$ spin-orbital components in Fc species. This could also be an evidence of successful grafting of b-Fc on TFC PA RO membrane.

The element contents of membranes and the ratio of C-O to C=O were presented in **Table 3.** The atomic concentration percent of Fe were higher than 5% in XPS data after modification while no Fe species were observed in neat membrane. Because there was no change of C=O composition in all process, the C=O content can be used as a reference. As correlated with the spectra, the ratio of C-O to C=O for membranes were calculated to be 0.39, 0.20, and 1.56 respectively. This showed the quantitative increase of C-O composition and indicated the presence of CD. To summarize the result, the b-Fc were modified onto the surface of TFC PA RO membrane and CDs were introduced, successfully.

Figure 11. XPS spectra of membrane samples

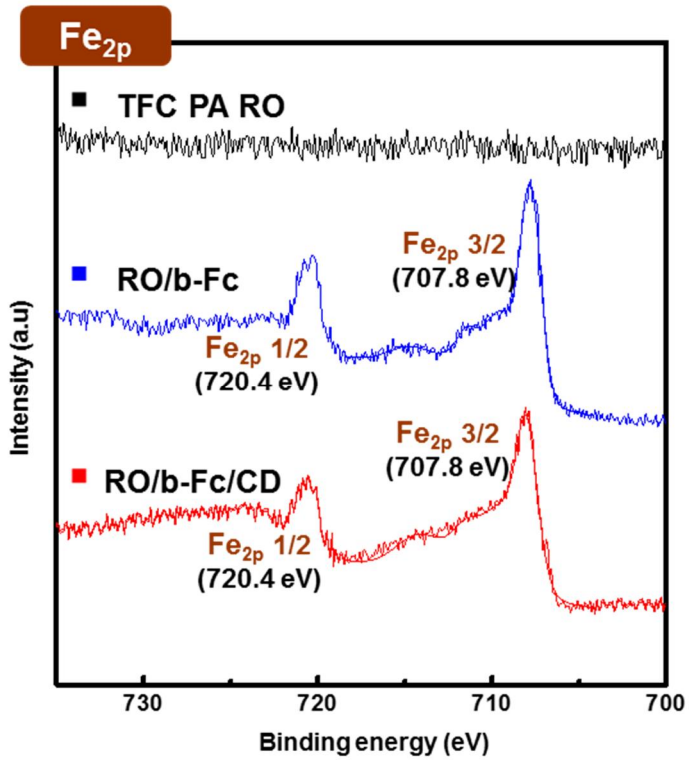

Figure 12. XPS spectra of membrane samples for iron species

	C (atomic conc. %)	N (atomic conc. %)	O (atomic conc. %)	Fe (atomic conc. %)	C-O/C=O ratio
TFC PA RO	74.48	7.66	17.72	-	0.39
RO/b-Fc	73.95	14.81	10.53	0.58	0.20
RO/b-Fc/CD	70.43	10.53	18.53	0.51	1.56

Table 3. Quantitative inspection result of XPS measurement for membrane samples

3.2.3. Surface morphology analysis

The morphological changes of the membrane surfaces were investigated by FE-SEM and AFM. The SEM observations were conducted with a magnification of 10,000 and 50,000. The FE-SEM images of the TFC PA RO, RO/b-Fc, and RO/b-Fc/CD were shown in **Figure 13**. The surface of TFC PA RO exhibited characteristic ridge-and-valley structure [36]. The modified membrane showed ridge-and-valley structure and no obvious difference between surface morphology of the virgin membrane. This indicated that the modification process occurred without any damage on membranes.

Figure 14 showed the images of three-dimensional 10 μm scans for unmodified and modified RO membranes. All membranes showed unique and characteristic ridge-and-valley structure. Moreover, according to the AFM results, the average roughness (Ra) of membranes were 42.33 nm, 41.82 nm, 54.79 nm and the root mean square roughness (Rq) were 53.88 nm, 52.90 nm, 69.66 nm, respectively. This was not notable difference and could conclude that the surface morphology of modified membrane was similar with unmodified membrane. The analytical results of AFM confirmed again that the b-FC/CD were successfully grafted on to the surface of commercial TFC PA RO membrane without damage.

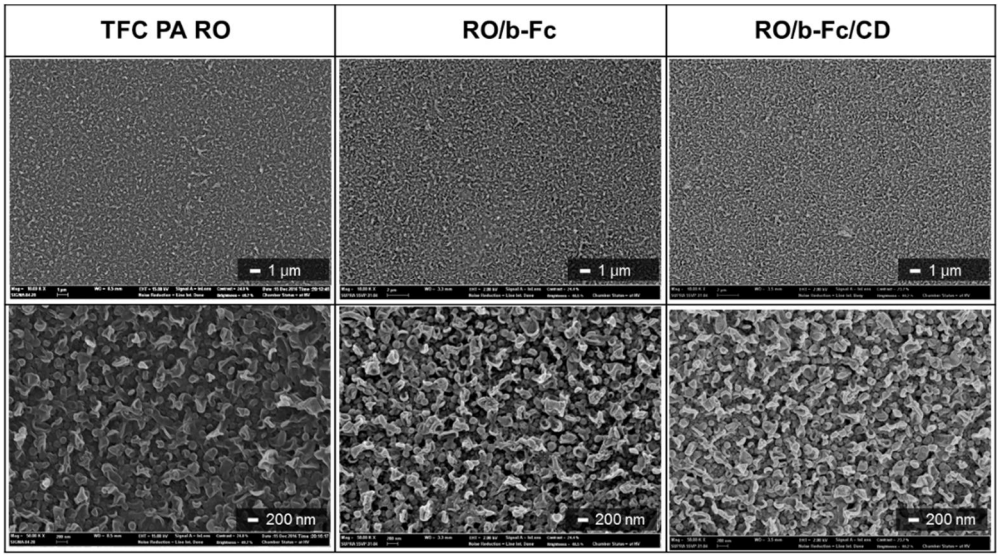

Figure 13. FE-SEM images of membrane samples

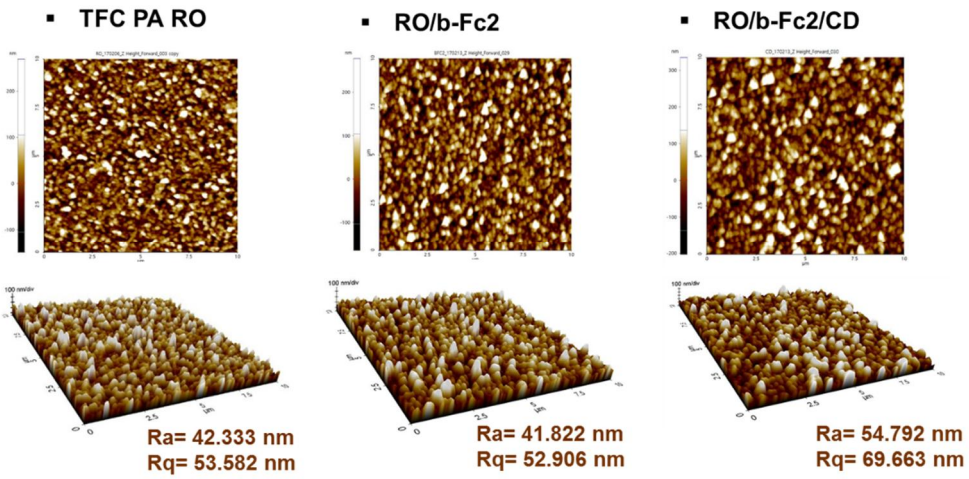

Figure 14. Three-dimensional AFM images of membrane samples

3.2.4. Contact angle analysis

Hydrophilicity is an important property of RO membrane because hydrophilic surfaces reduce the fouling of various hydrophobic foulants. The hydrophilic property of the membrane surfaces were characterized by water contact angle measurement. **Figure 15** showed contact angle of TFC PA RO, RO/b-Fc, and RO/b-Fc/CD. The water contact angle of TFC PA RO was 32.1° and after modification with b-Fc, the water contact angle slightly increased to 33.8°. Despite of hydrophilicity of b-PEI, ferrocene had high hydrophobic property so the total hydrophilicity of RO/b-Fc surface was decreased. On the other hand, the surface of RO/b-Fc/CD had a water contact angle value of 13.5° which had the highest hydrophilicity. This was because the hydrophobic cavity of cyclodextrin hindered the ferrocene by composing the complex, and the hydrophilic surface of hydroxyl group in cyclodextrin appeared on the membrane surface. In conclusion, the water contact angle was changed from 32.1° to 13.5° after b-Fc/CD modification and the decrease of the contact angle value revealed that hydrophilicity of membrane surface increased due to the hydrophilic nature of b-PEI and hydrophilic surface of CD.

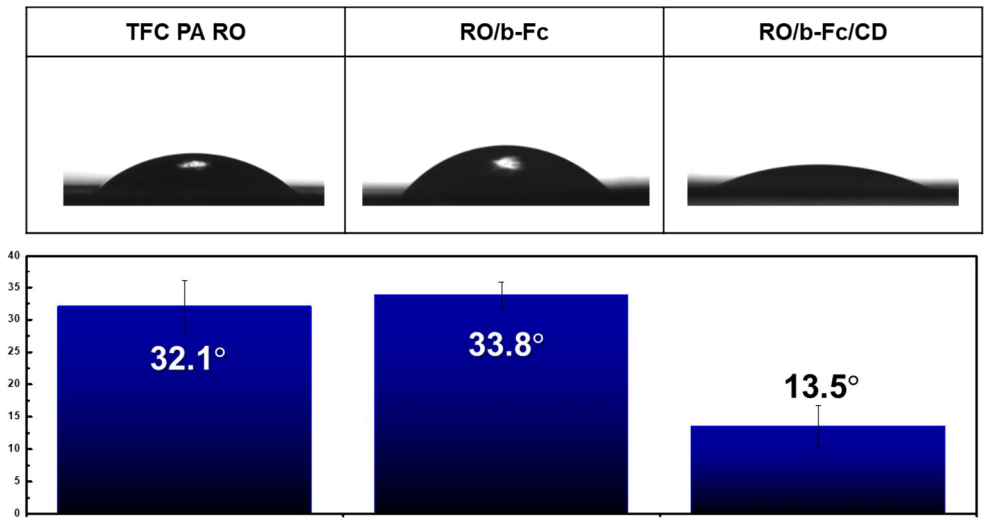

Figure 15. The static contact angles of membrane samples

3.3. Comparison in different composition of b-Fc

3.3.1. XPS and DLS analysis

To compare the membranes with different composition of b-Fc, RO/b-Fc1/CD, RO/b-Fc2/CD, RO/b-Fc4/CD, and RO/b-Fc6/CD were characterized by XPS. **Figure 16** showed the high resolution XPS spectra of C_{1s} and O_{1s} of RO/b-Fc/CD with various composition of b-Fc. All RO/b-Fc/CD membranes showed high intensity of C-O peak which indicated the successful introduction of CD. With increasing concentration of ferrocene in b-Fc, the C-O peak became more distinct due to increasing of cyclodextrin.

The relative amounts of cyclodextrin, the intensity of b-Fc, and number of cyclodextrin per b-Fc were calculated by XPS spectra. Because there was no difference in C=O of O_{1s} spectra in the course of the experiment, Atomic percentage of C=O was used as reference. The comparison of calculated results were shown in **figure 16** using following equations. The number of C-O in CD was 35 and number of N in b-Fc (Mw: 25000) was about 582

The relative amounts of cyclodextrin:

$$\frac{\text{Atomic \% of C-O in RO/b-Fc/CD}}{\text{Atomic \% of C=O in RO/b-Fc/CD}} - \frac{\text{Atomic \% of C-O in RO/b-Fc}}{\text{Atomic \% of C=O in RO/b-Fc}} \qquad (3)$$

The relative amounts of b-Fc:

$$\frac{\text{Atomic \% of N in RO/b-Fc}}{\text{Atomic \% of C=O in RO/b-Fc}} - \frac{\text{Atomic \% of N in TFC PA RO}}{\text{Atomic \% of C=O in TFC PA RO}} \quad (4)$$

The number of cyclodextrin per b-Fc:

$$\frac{\text{Intensity of cyclodextrin / Number of C-O in CD}}{\text{Intensity of b-Fc / Number of N in b-PEI}} \quad (5)$$

The result indicated that the intensity of cyclodextrin increased 0.88 to 2.08 as the composition of ferrocene in b-Fc increased. Also, the intensity of b-Fc increased dramatically in RO/b-Fc6/CD than other compositions of ferrocene. The number of cyclodextrin per b-Fc showed 15.36 in RO/b-Fc1/CD and saturated as about 22 in higher ratio of ferrocene in b-Fc. In other words, the number of cyclodextrin that could be introduced to b-Fc were limited to about 22 and this result confirmed that the total cyclodextrin on membrane increased not by combining with all ferrocene efficiently, but by increasing of b-Fc introduced on membrane.

The introduction of large amounts of b-Fc on TFC PA RO can explained by DLS. In **figure 17**, the size of b-Fc1 and b-Fc2 were about 10 nm which was the similar size with b-PEI. On the other hand, the size of b-Fc4 and b-Fc6 were 63.6 nm and 104.3 nm, respectively. The cause of bigger size was hydrophobic property of ferrocene that reduced the dispersion uniformity, so the larger aggregation appeared. By the hydrophobic property

of ferrocene, the solution of b-Fc in D.I water got more opaque as composition of ferrocene increased. So, after grafting b-Fc on RO membrane, the additional b-Fc was introduced in addition to the b-Fc bonded to the carboxyl group at high composition of ferrocene. This result indicated that controlling the amount of ferrocene to b-PEI was necessary for efficient grafting of b-Fc on TFC PA RO. The solution of b-Fc series and scheme after grafting b-Fc series on TFC PA RO were shown in **figure 18**.

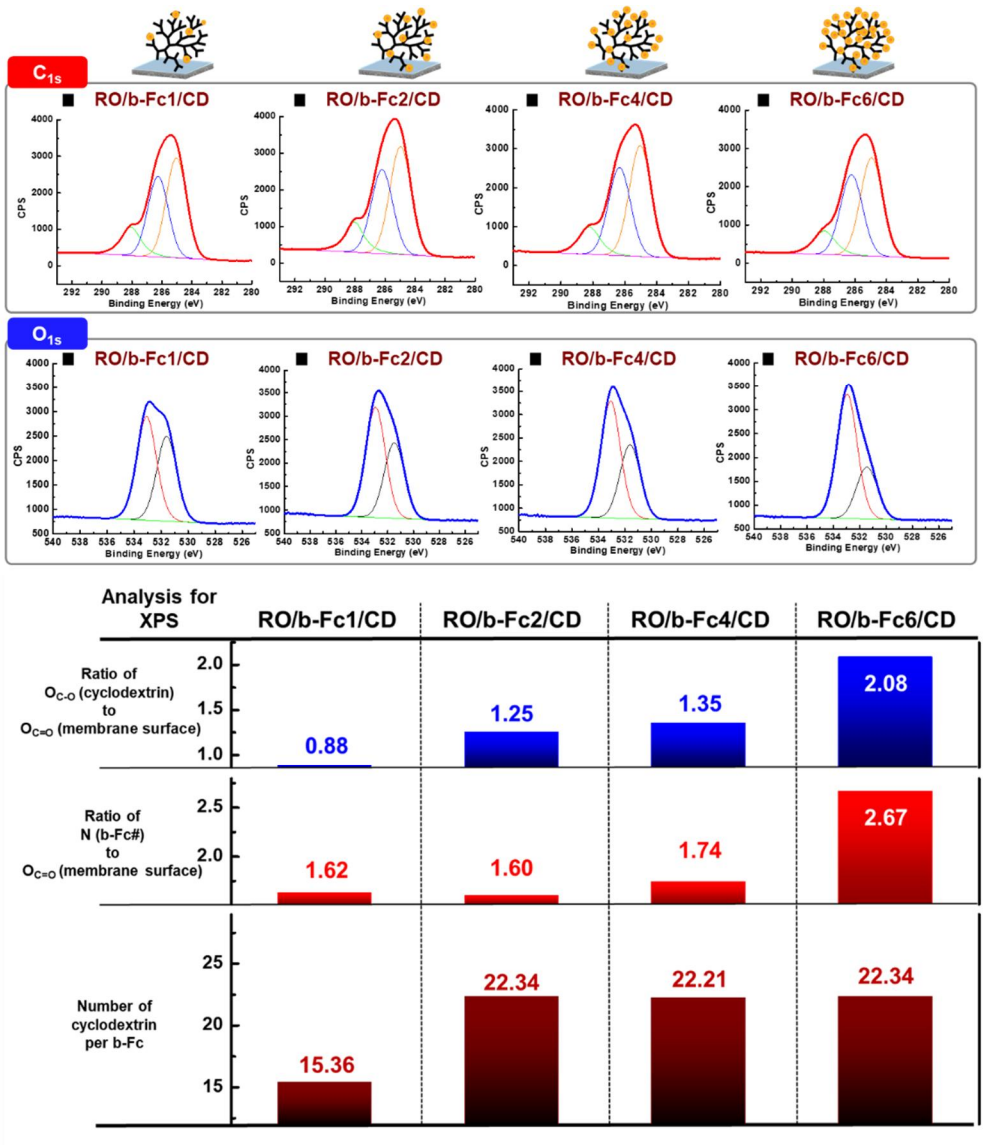

Figure 16. XPS spectra of membrane samples with different compositions and calculated results about intensity of cyclodextrin, intensity of b-Fc, and number of cyclodextrin per b-Fc

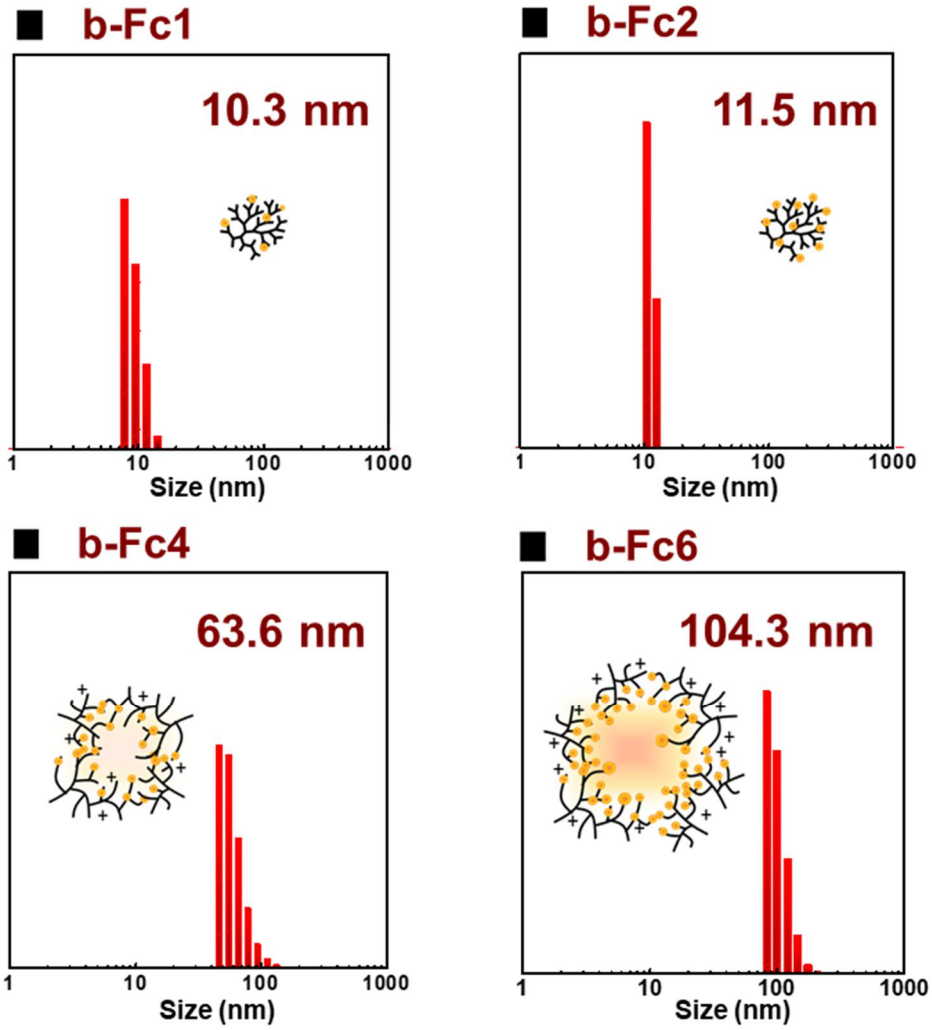

Figure 17. The DLS results of membrane samples

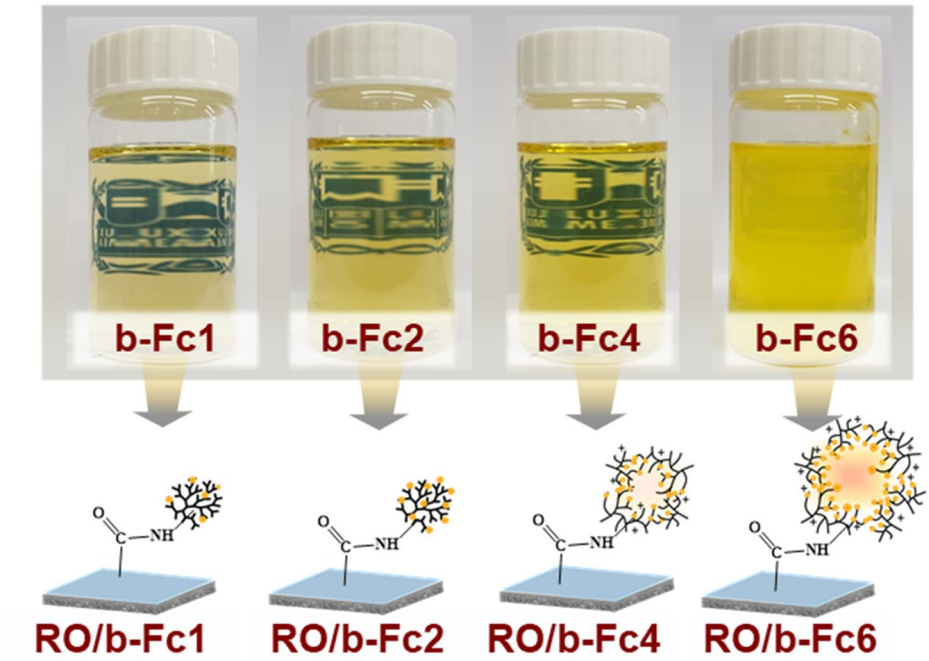

Figure 18. The solution of b-Fc1, b-Fc2, b-Fc4, and b-Fc6 and scheme after grafting b-Fc series on TFC PA RO

3.3.2. Contact angle analysis

The change of hydrophilicity of membrane surface was characterized by water contact angle measurement with different composition of ferrocene in b-Fc. **Figure 19** showed contact angle of RO/b-Fc series and RO/b-Fc/CD series at various composition. As concentration of ferrocene in b-Fc increased, the contact angle increased gradually from 15.9° to 55.3° which was the effect of the increase in ferrocene. After introduction of CDs, the contact angle decreased in all membranes which indicated the hydrophilicity of surface increased due to hydrophilic surface of cyclodextrin and hiding of hydrophobic ferrocene. The contact angle of RO/b-Fc/CD series was about 9.5°, 11.8°, 13.5°, and 39.5°, respectively. The point was that RO/b-Fc6/CD showed relatively high contact angle than other membranes after introduction of CD. This could explained by XPS analysis data (Fig 16) that number of cyclodextrin in one b-Fc had limitation. In other words, there were much ferrocene that did not form a complex with cyclodextrin in high composition of ferrocene. So high hydrophobic surface property appeared on RO/b-Fc6/CD. As the result, Adjusting composition of ferrocene was necessary to get hydrophilic surface and introduce the cyclodextrin efficiently on the membrane.

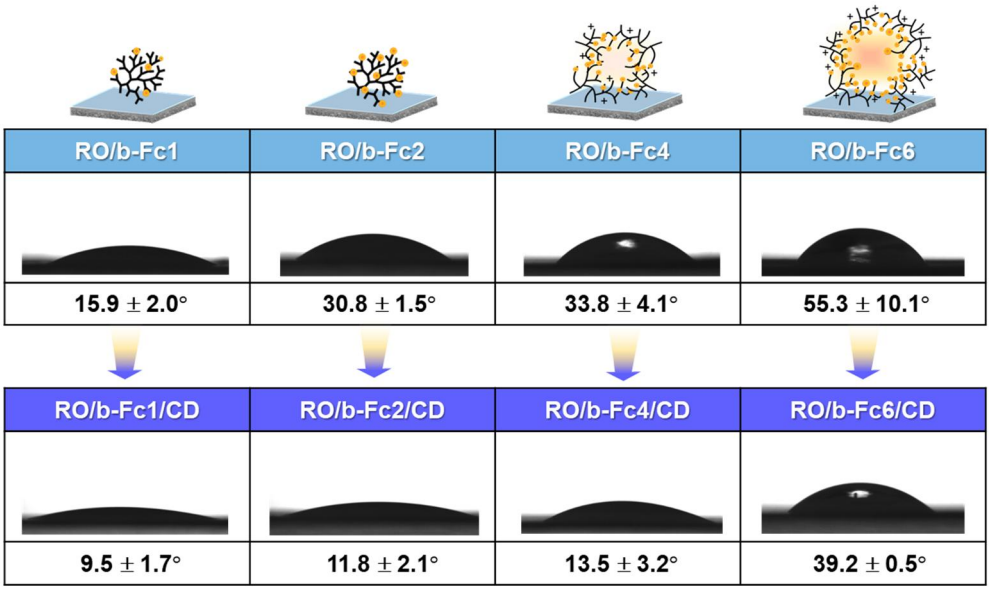

Figure 19. The static contact angles of membrane samples with different compositions

3.4. Regeneration of CDs through electrical treatment

3.4.1. Metal plate electrode

The surface of RO/b-Fc/CD membrane possessed cyclodextrins connected with ferrocene. As the ferrocene and cyclodextrin complex could dissociate with oxidation of ferrocene, the surface CDs of RO/b-Fc/CD performed detaching and attaching reaction by electrical treatment. For electrical treatment, metal plates of aluminum, copper, and titanium were used as electrode. The electrical treatment proceeded in 0.5M NaCl solution for 30s and RO/b-Fc/CD membrane was located on anode. First, aluminum was used as electrodes. During the experiment, aluminum oxide was generated at the anode. The following equations showed the reaction on anode

$$2Al \rightarrow 2Al^{3+} + 6e^{-}$$

$$2Al^{3+} + 3H_2O \rightarrow Al_2O_3 + 6H^{+}$$

With other metal plates like copper and titanium, same results were obtained. As shown in **figure 20**, ATR-FTIR peak of membrane after electrical treatment represented the contamination of membrane by metal oxide when used aluminum and titanium. In the case of copper, the color of the membrane was completely changed to brown by the copper oxide. These results indicated that metals were not suitable for this experiment.

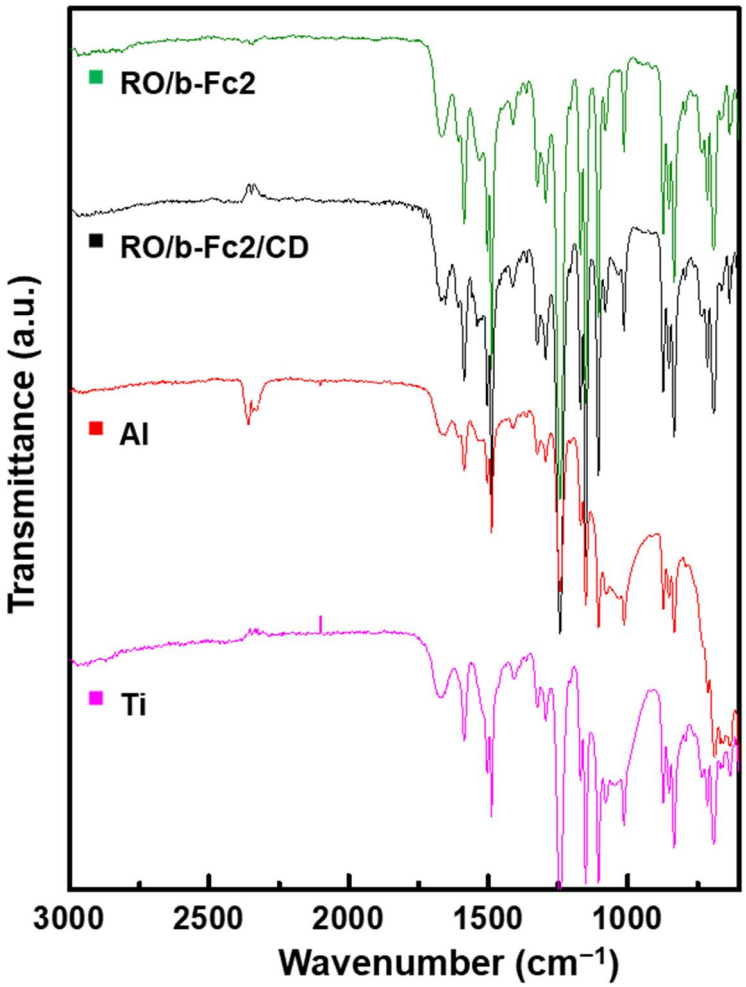

Figure 20. ATR-FTIR spectra of RO/b-Fc/CD membranes after electrical treatment using metal electrode

3.4.2. Carbon plate electrode

Carbon plate was widely used as an electrode material in electrochemistry. Carbon plate had lower electrical conductivity than metal like copper, but did not generate metal oxides. To prevent the generation of metal oxide, electrode changed metal plate to carbon plate. The experimental conditions proceeded in 0.5M NaCl solution for 30s both in oxidation and reduction condition which was same as metal electrode experiment.

ATR-FTIR spectra was used to evaluate the successful detachment and re-attachment of CDs from the surface of RO/b-Fc/CD. The presence of cyclodextrin was determined according to the presence or absence of the peak of C-O stretch in glucose ring of cyclodextrin at 1038 cm^{-1}. In **figure 21**, C-O stretch was vanished clearly after electrical treatment using carbon plate as anode. This confirmed that the CDs detached from the membrane by oxidation of ferrocene without contamination. This membrane was named as RO/b-Fc*. For re-attaching the CDs, same experiment was conducted on carbon plate as cathode. After reduction, membrane was immersed in an aqueous solution of β-cyclodextrin for overnight. Then the membrane was draw out and washed with deionized water. This membrane was named as R-RO/b-Fc/CD. R-RO/b-Fc/CD membrane showed appearance of C-O stretch peak at 1038 cm^{-1} in **figure 21**, which indicated that cyclodextrin was reintroduced properly by forming the complex with reduced ferrocenium. To

summarize, RO/b-Fc/CD was successfully regenerated by detaching and re-attaching CDs using carbon plate as electrode.

XPS analysis provided more detailed information about regeneration of the CDs. The XPS spectrum of C_{1s} and O_{1s} was portrayed in **figure 22**. For RO/b-Fc* membrane sample, the intensity of C-O peak at 286.5 eV in high resolution C_{1s} spectra and at 533.0 eV in high resolution O_{1s} spectra was dramatically decreased. This indicated the successful detachment of CDs from the membrane by electrical treatment. After reduction the membrane and reintroduction of CDs, the intensity of C-O in R-RO/b-Fc/CD membrane was recovered by the attachment of CDs on membrane surface. Also, the Fe_{2p} spectrum was showed in **figure 23**. The peaks at 707.8 and 720.4 eV corresponding to binding energy of $2p_{2/3}$ and $2p_{1/2}$ spin-orbital components of ferrocene shifted to 709.7 and 723.1 eV by oxidation of ferrocene. And the Fe_{2p} spectrum of R-RO/b-Fc/CD showed that the peak of ferrocene recovered which confirmed the successful reduction of ferrocene. Through the XPS quantitative analysis, the changes in the amount of cyclodextrin were confirmed. In **table 4**, the ratio of C-O to C=O decreased from 1.43 to 0.53 and recovered as 1.37 which presented the absence and presence of CD. The combined results of XPS were demonstrated that the oxidation of ferrocene produced a repulsive force caused the CDs to fall off the membrane surface and by reducing the ferrocene, the CDs could be

formed on the membrane surface through recombination with ferrocene since the ferrocene was restored to its hydrophobicity. This way, the RO/b-Fc/CD was successfully regenerated.

Finally, contact angle measurement was performed to evaluate the change of membrane hydrophilicity according to the presence of CDs. **Figure 24** showed the change of water contact angle according to the electrical experimental step. The water contact angle of RO/b-Fc/CD was 11.8° and after oxidation of membrane, the value of contact angle increased to 29.7°. This is because the CDs disappeared on the surface and the hydrophobic ferrocene was exposed. So, the water contact angle of RO/b-Fc* was almost corresponded with the value of RO/b-Fc in **figure 15**. After re-attachment of CDs, the contact angle was recovered. This showed that the hydrophilic property of the surface was restored by the regeneration of the CDs using the electrical treatment.

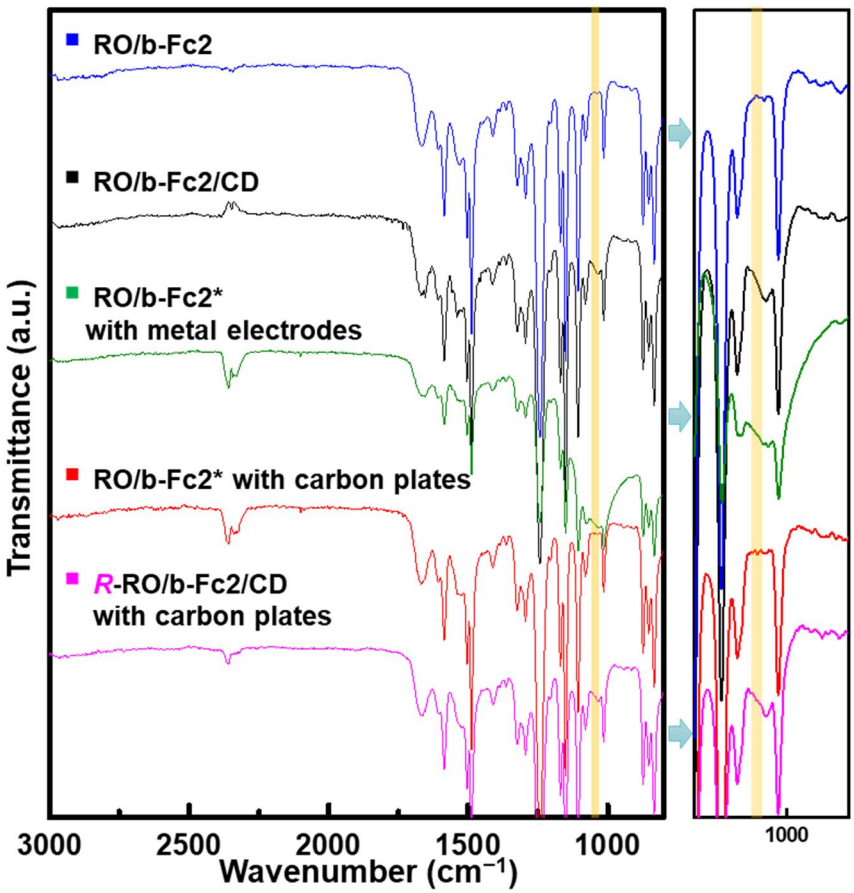

Figure 21. ATR-FTIR spectra of RO/b-Fc/CD membranes after electrical treatment using carbon plate

Figure 22. XPS spectra of RO/b-Fc/CD, RO/b-Fc*, and R-RO/b-Fc/CD

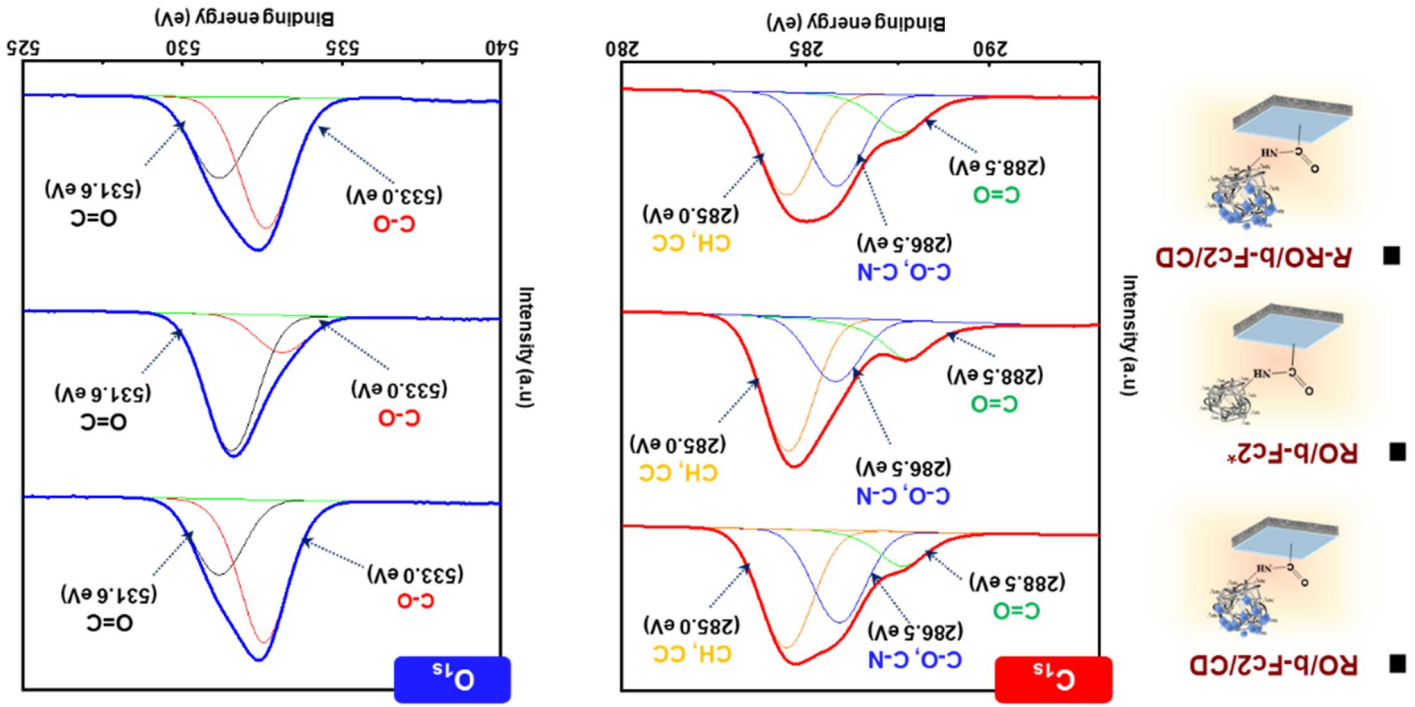

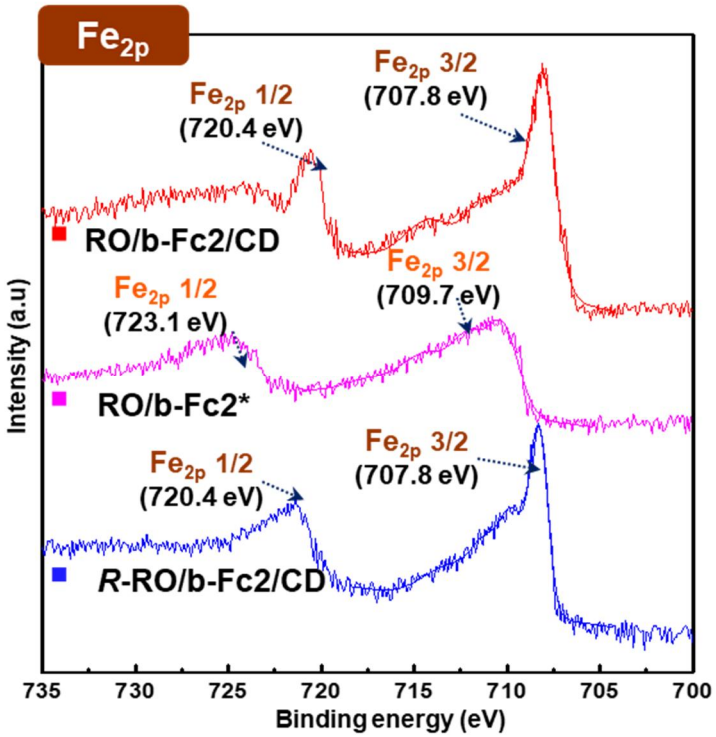

Figure 23. XPS spectra of RO/b-Fc/CD, RO/b-Fc*, and RO/b-Fc/CD for iron species

	C (atomic conc. %)	N (atomic conc. %)	O (atomic conc. %)	Fe (atomic conc. %)	C-O/C=O ratio
RO/ b-Fc2/CD	71.51	11.06	17.25	0.34	1.43
RO/b-Fc2*	72.12	10.59	17.19	0.15	0.53
R-RO/ b-Fc2/CD	68.89	10.12	19.84	0.31	1.37

Table 4. Quantitative inspection result of XPS measurement for RO/b-Fc/CD, RO/b-Fc*, and R-RO/b-Fc/CD

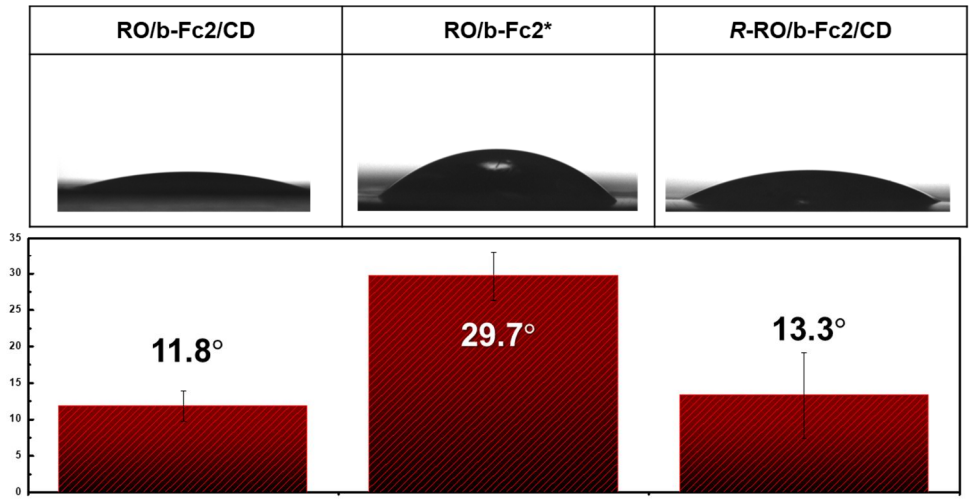

Figure 24. The static contact angles of RO/b-Fc/CD, RO/b-Fc*, and R-RO/b-Fc/CD

3.5. Performance evaluation

3.5.1. Pure water flux and rejection

The pure water flux and NaCl rejection of TFC PA RO membrane and RO/b-Fc/CD membranes were presented in **figure 25**. The performance was carried out at 14 bar and RT. The salt rejections of RO/b-Fc/CD membranes showed no significant change after modification. This was because, the grafting method in this experiment was conducted in a mild aqueous environment without any drying process or damaging effect unlike some other grafting methods such as UV-initiated polymerization or plasma polymerization. The experiment process was operated in simple and mild way, So NaCl removal rate of modified membranes could be maintained at a value of commercial polyamide RO membrane which was about 96% or more.

Two factors were effected on the water permeation. One is the increased trans-membrane resistance of water molecule and the other is hydrophilicity of membrane surface which could facilitate the solution-diffusion process of water molecule on membrane. The final value depended on which factor dominated. As compared with the virgin membrane, the water flux of RO/b-Fc/CD membranes decreased with increasing of

ferrocene concentration obviously which showed the effect of trans-membrane resistance became the dominated factor.

As described in **figure 17** by DLS result, b-Fc4 and b-Fc 6 had larger size than b-Fc1 and b-Fc2. So, RO/b-Fc4/CD and RO/b-Fc6/CD had the greater resistance to water molecule and water permeability reduced by about 68% and 60% from the TFC PA RO membrane, respectively. RO/b-Fc1/CD and RO/b-Fc2/CD, on the other hand, exhibited a fairly high water permeability which was about 80% that of TFC PA RO membrane due to low resistance to water of small size of b-Fc1 and b-Fc2. Among the membranes having high water permeability, RO/b-Fc2/CD had a larger amount of CD on the surface than RO b-Fc1/CD (**figure 16**) and therefore it was considered to be the most suitable membrane to confirm the recovery performance by electrical treatment. In conclusion, RO/b-Fc2/CD had a high water permeability and a large amount of CD, so it was the most adapted regeneration membrane for fouling control.

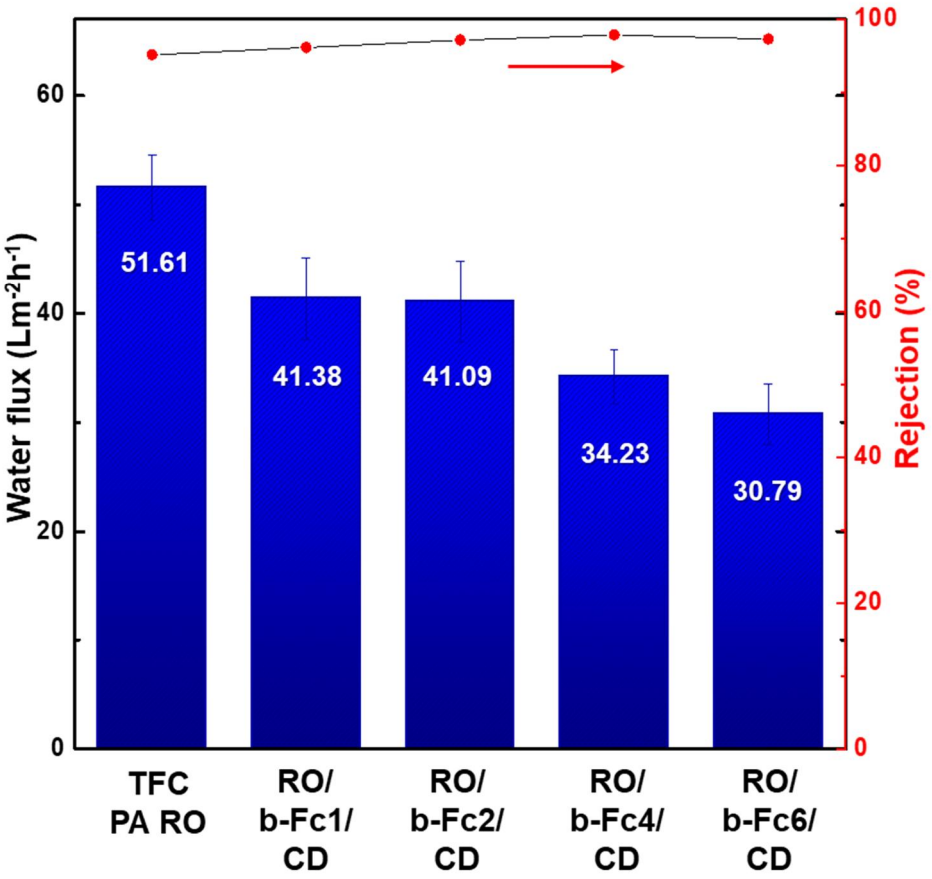

Figure 25. The water fluxes and salt rejections of the TFC PA RO membrane and RO/b-Fc/CD membranes

3.5.2. CTAC filtration

Filtration test was conducted using RO/b-Fc2/CD with high water permeability, hydrophilicity, and a large amount of cyclodextrins, as previously described. CTAC, a typical foulant in wastewater, was selected to evaluate anti-fouling performance. After filtration, membranes were immersed in D.I water for washing. The TFC PA RO membranes with cleaning solution and water washing were used as a comparison group.

The filtration result was showed in **figure 26**. When the 60 mg/L of CTAC solution was poured, the water flux of TFC PA RO rapidly decreased to about 18% at the initial stage. In contrast, the water flux of the RO/b-Fc2/CD slowly declined to 56% after 120 minute investigation. It indicated that the decreased water flux of RO/b-Fc2/CD caused by CTAC fouling were less than that of the TFC PA RO membrane. After the pure water washing, the water flux for TFC PA RO was recovered to 31% and maintained low water flux in repeated filtration experiments even after water washing. While the recovered flux of RO/b-Fc2/CD was 78% of initial flux and showed successive high restoration of water flux after three times of filtration test. Compared with pure water washing, TFC PA RO with cleaning solution showed higher recovery of water flux which was about 46%. But, in repeated process, the recovery rate of water flux by the cleaning solution was reduced and eventually TFC PA RO with cleaning solution had a low water flux

similar to that of using pure water washing. In conclusion, RO/b-Fc2/CD itself had a better and more reversible restoration of water flux even after simple D.I water cleaning than neat membrane with cleaning solution, and showed good anti-fouling property due to membrane hydrophilicity.

The quantitative calculations were conducted to analyze the flux recovery performance with specific values of fouling test using CTAC solution. Flux recovery ratio (FRR) was analyzed with normalized flux of TFC PA RO membrane with water washing and NaOCl cleaning, and RO/b-Fc2/CD membrane. FRR was calculated as following equation (6).

$$\mathbf{FRR}\ (\%) = \frac{J_R}{J_0} \times \mathbf{100} \qquad (6)$$

Where J_R was the water flux of cleaned membrane and J_0 was the initial water flux. In **figure 27**, FRR of TFC PA RO with cleaning solution increased than that of TFC PA RO with water washing. But, RO/b-Fc2/CD had 77.4% of FRR which was the highest value and indicated that RO/b-Fc2/CD had good resistance and easy recovery to fouling.

To discuss the degree of membrane fouling, reversible and irreversible fouling resistance (R_r, R_{ir}) of membranes were calculated as following equations (7) and (8).

$$\mathbf{R_r} = \frac{J_R - J_p}{J_0} \times \mathbf{100} \qquad (7)$$

$$\mathbf{R_{ir}} = \frac{J_0 - J_R}{J_0} \times \mathbf{100} \quad (8)$$

Where Jp was the flux of foulant solution. TFC PA RO with water washing had low reversible fouling resistance and high irreversible fouling resistance which was about 9.7% and 70.2%, respectively. By using cleaning solution, R_{ir} of membrane decreased to 56% and RO/b-Fc2/CD showed the lowest value of R_{ir} as 22.6%. This low value of R_{ir} confirmed that RO/b-Fc2/CD had high antifouling property.

3.5.3. Comparison of cleaning efficiency

After three cycle filtration tests, electrical treatment was applied for regeneration effect. Membranes were oxidized and reduced for 30s and immersed in cyclodextrin solution overnight. Through the regeneration experiment, the contaminated CDs could be replaced with a new CDs. With TFC PA RO membrane that had no b-Fc/CD on the surface, the same regeneration procedure was carried out for comparison. Cleaning efficiency of membranes were compared after regeneration experiment.

As shown in **figure 26**, the normalized water flux of TFC PA RO with water washing and NaOCl cleaning showed no significant change after the electrical treatment. On the other hand, the normalized water flux of RO/b-Fc2/CD recovered greatly. Quantitative calculations using equation (6),

(7), and (8) were performed for a more accurate analysis. The result was described in **figure 28**. 86.4% of its original performance was recovered after electrical treatment process in RO/b-Fc2/CD membrane which was higher than that of RO/b-Fc2/CD with pure water washing. This result indicated the water flux of membrane could be recovered from fouling by regeneration of CDs. In the case of R_{ir}, TFC PA RO with water washing and NaOCl cleaning after electrical treatment represented a high value of 81.6% and 72.9%, respectively. But, RO/b-Fc2/CD after regeneration of CDs had a significantly lower R_{ir} value of 13.6% which was even smaller than with water washing. This was attributed to the fact that the permanently fouling of CTAC was eliminated from the membrane together with the CDs. In conclusion, regeneration of CDs was highly effective for water flux recovery from fouled membrane.

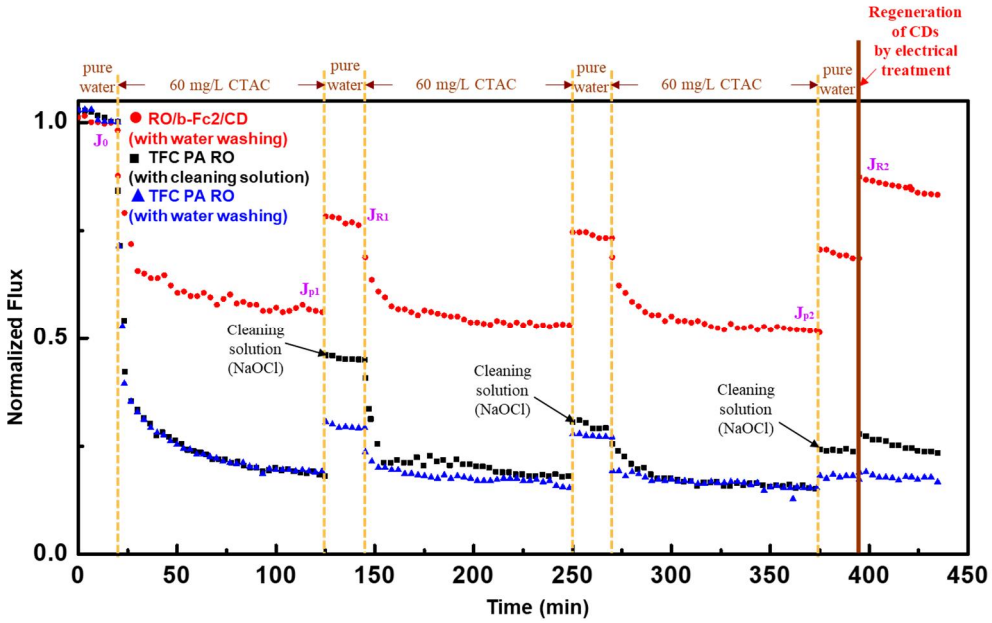

Figure 26. Membrane filtration test result with CTAC solution of TFC PA RO and RO/b-Fc2/CD

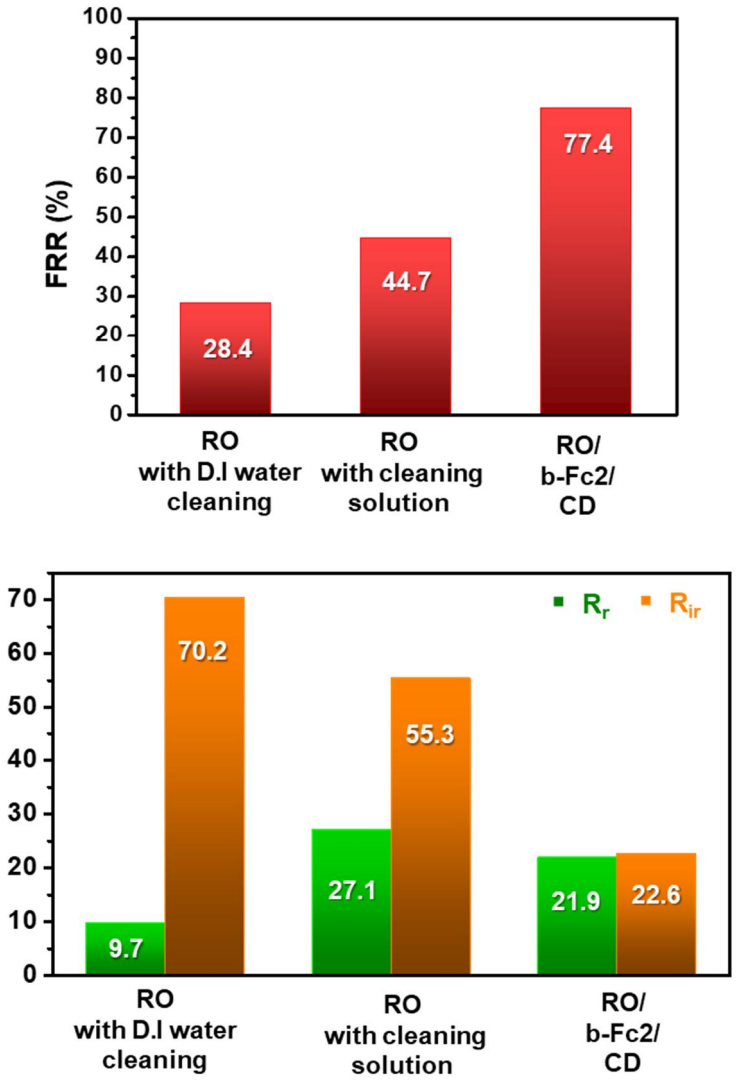

Figure 27. Quantitative analysis of CTAC filtration test result

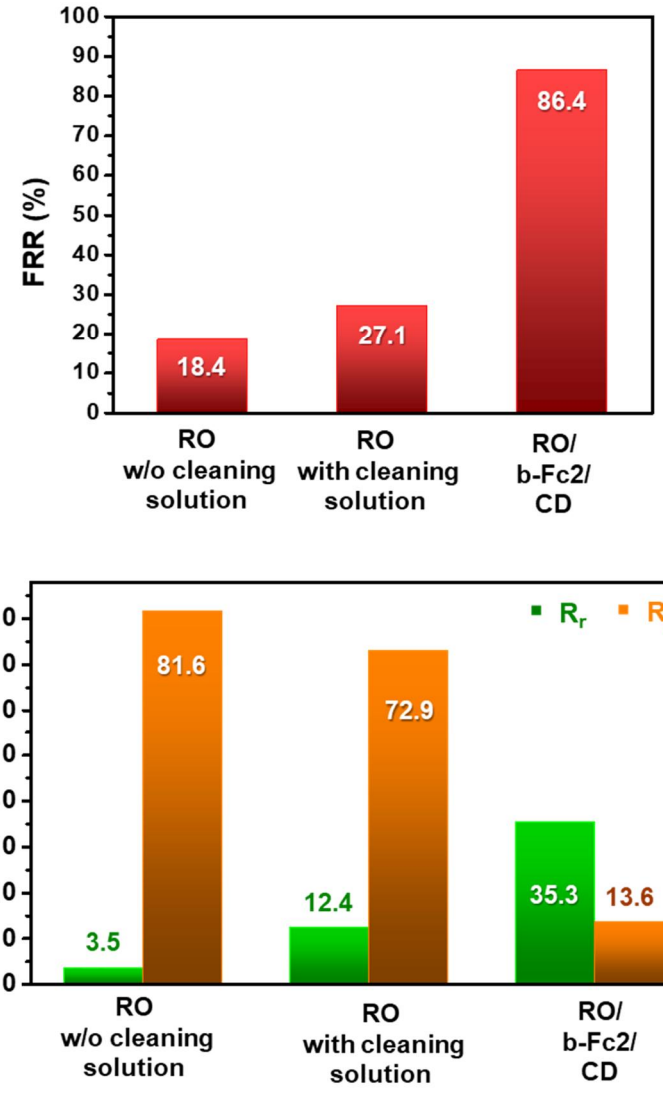

Figure 28. Quantitative analysis of cleaning efficiency test result

4. Conclusion

In this research, we developed regenerable reverse osmosis membrane to control the fouling using electro-responsive ferrocene-cyclodextrin complex on hydrophilic b-PEI. Initially, b-Fc were synthesized by b-PEI and ferrocene with various compositions to optimize the amount of ferrocene. FT-IR and H^1NMR study confirmed the successful synthesis of Fc and molar ratio of Fc and b-PEI. Synthesized b-Fc samples were attached to commercial reverse osmosis membrane by EDC, NHS-induced grafting and cyclodextrin was introduced on it. Fabricated RO/b-Fc/CD membranes were characterized by ATR-FTIR, XPS, FE-SEM, AFM, and contact angle measurement. Successful grafting of b-Fc and introduction of CD were observed. With the comparison of various composition by XPS, DLS, and contact angle measurement, we found that overconsolidation of b-Fc occurred as the composition of b-Fc increased. Water flux was greatly reduced due to this aggregation phenomenon, and therefore, RO/b-Fc2/CD was defined as an optimized membrane which had high water flux by no aggregation and large amount of CD. The NaCl rejection of membranes which were higher than 96% proved that RO performance was maintained after modification.

ATR-FTIR, XPS, and water contact angle measurement confirmed

the attaching and detaching of CDs and proved successful regeneration of CDs by using carbon plate. Then, Water filtration test by CTAC solution was performed to measure the antifouling property of RO/b-Fc2/CD membrane. Antifouling property of RO/b-Fc2/CD membrane was enhanced about 49% than RO with pure water cleaning and 32.7% than RO with cleaning solution. Finally, cleaning efficiency was determined by CTAC filtration test after electrical treatment to replace the contaminated CDs to new one. The water flux of RO/b-Fc2/CD recovered to 86.4% after regeneration of CDs and had low value of irreversible fouling resistance. This showed that regeneration of CDs was effective way to recover the water flux after contamination.

As a result, RO/b-Fc2/CD had high antifouling property by hydrophilicity and cleaning efficiency by regeneration of CDs compared to TFC PA RO membrane. Therefore, RO/b-Fc2/CD membrane could be used at application of water desalination in place of commercial RO membrane. By using carbon sheet as spacer for electrode, membrane could be regenerated and it could give economic and environmental efficiency on water desalination industry.

References

[1] Hightower, Mike, and Suzanne A. Pierce. "The energy challenge." *Nature*452.7185 (2008): 285-286.

[2] Bartman, Alex R., et al. "Mineral scale monitoring for reverse osmosis desalination via real-time membrane surface image analysis." *Desalination*273.1 (2011): 64-71.

[3] Ochando-Pulido, J. M., M. D. Victor-Ortega, and A. Martínez-Ferez. "On the cleaning procedure of a hydrophilic reverse osmosis membrane fouled by secondary-treated olive mill wastewater." *Chemical Engineering Journal* 260 (2015): 142-151.

[4] Tang, Fang, et al. "Fouling characteristics of reverse osmosis membranes at different positions of a full-scale plant for municipal wastewater reclamation." *Water research* 90 (2016): 329-336.

[5] Misdan, Nurasyikin, W. J. Lau, and A. F. Ismail. "Seawater Reverse Osmosis (SWRO) desalination by thin-film composite membrane—Current development, challenges and future prospects." *Desalination* 287 (2012): 228-237.

[6] Lau, W. J., et al. "A recent progress in thin film composite membrane: a review." *Desalination* 287 (2012): 190-199.

[7] Fritzmann, C., et al. "State-of-the-art of reverse osmosis

desalination." *Desalination* 216.1-3 (2007): 1-76.

[8] Rana, Dipak, and Takeshi Matsuura. "Surface modifications for antifouling membranes." *Chemical reviews* 110.4 (2010): 2448-2471.

[9] Kang, Guodong, et al. "Surface modification of a commercial thin film composite polyamide reverse osmosis membrane by carbodiimide-induced grafting with poly (ethylene glycol) derivatives." *Desalination* 275.1 (2011): 252-259.

[10] Xu, Jun, et al. "Positively charged aromatic polyamide reverse osmosis membrane with high anti-fouling property prepared by polyethylenimine grafting." *Desalination* 365 (2015): 398-406.

[11] Zhou, Yong, et al. "Surface modification of thin film composite polyamide membranes by electrostatic self deposition of polycations for improved fouling resistance." *Separation and Purification Technology* 66.2 (2009): 287-294.

[12] Tokarev, Ihor, et al. "Stimuli-responsive hydrogel membranes coupled with biocatalytic processes." *ACS applied materials & interfaces* 1.3 (2009): 532-536.

[13] Wandera, Daniel, S. Ranil Wickramasinghe, and Scott M. Husson. "Stimuli-responsive membranes." *Journal of Membrane Science* 357.1 (2010): 6-35.

[14] Han, Chun-Chieh, et al. "Temperature-responsive poly (tetrafluoroethylene) membranes grafted with branched poly (N-isopropylacrylamide) chains." *Journal of Membrane Science* 358.1 (2010): 60-66.

[15] Wang, Guan, et al. "Thermo□Responsive Polyethersulfone Composite Membranes Blended with Poly (N□isopropylacrylamide) Nanogels." *Chemical Engineering & Technology* 35.11 (2012): 2015-2022.

[16] Himstedt, Heath H., Kathryn M. Marshall, and S. Ranil Wickramasinghe. "pH-responsive nanofiltration membranes by surface modification." *Journal of membrane science* 366.1 (2011): 373-381.

[17] Ilyas, Shazia, et al. "Multifunctional polyelectrolyte multilayers as nanofiltration membranes and as sacrificial layers for easy membrane cleaning." *Journal of colloid and interface science* 446 (2015): 386-393.

[18] Liu, Zhuang, et al. "Positively K+□responsive membranes with functional gates driven by host–guest molecular recognition." *Advanced Functional Materials*22.22 (2012): 4742-4750.

[19] Himstedt, Heath H., et al. "Toward remote-controlled valve functions

via magnetically responsive capillary pore membranes." *Journal of membrane science* 423 (2012): 257-266

[20] Steehler, J. K., et al. "Electric field induced permeability modulation in pure and mixed Langmuir-Blodgett multilayers of hemicyanine dyes and octadecanoic acid on nanoporous solid supports." *Journal of membrane science* 139.2 (1998): 243-257.

[21] Park, Sung Yong, Jae Woo Chung, and Seung-Yeop Kwak. "Regenerable anti-fouling active PTFE membrane with thermo-reversible “peel-and-stick” hydrophilic layer." *Journal of Membrane Science* 491 (2015): 1-9.

[22] Ahmadiannamini, Pejman, Merlin L. Bruening, and Volodymyr V. Tarabara. "Sacrificial polyelectrolyte multilayer coatings as an approach to membrane fouling control: disassembly and regeneration mechanisms." *Journal of Membrane Science* 491 (2015): 149-158.

[23] Kang, Yan, et al. "Regenerable Polyelectrolyte Membrane for Ultimate Fouling Control in Forward Osmosis." *Environmental Science & Technology* 51.6 (2017): 3242-3249.

[24] Chuo, Tsai-Wei, et al. "Electrically driven biofouling release of a poly (tetrafluoroethylene) membrane modified with an electrically induced reversibly cross-linked polymer." *ACS applied materials & interfaces* 5.20 (2013): 9918-9925.

[25] Takashima, Yoshinori, et al. "Expansion–contraction of photoresponsive artificial muscle regulated by host–guest interactions." *Nature communications* 3 (2012): 1270.

[26] Wang, Jing, and Ming Jiang. "Polymeric self-assembly into micelles and hollow spheres with multiscale cavities driven by inclusion complexation." *Journal of the American Chemical Society* 128.11 (2006): 3703-3708.

[27] Peng, Liao, et al. "Ferrocene-based supramolecular structures and their applications in electrochemical responsive systems." *Chemical Communications* 50.86 (2014): 13005-13014.

[28] Harada, Akira. "Cyclodextrin-based molecular machines." *Accounts of Chemical Research* 34.6 (2001): 456-464.

[29] Yan, Qiang, et al. "Voltage-responsive vesicles based on orthogonal assembly of two homopolymers." *Journal of the American Chemical Society* 132.27 (2010): 9268-9270.

[30] Dick, C. R., and G. E. Ham. "Characterization of polyethylenimine." *Journal of Macromolecular Science—Chemistry* 4.6 (1970): 1301-1314.

[31] Sun, Shi Peng, T. Alan Hatton, and Tai-Shung Chung. "Hyperbranched polyethyleneimine induced cross-linking of polyamide− imide nanofiltration hollow fiber membranes for

effective removal of ciprofloxacin." *Environmental science & technology* 45.9 (2011): 4003-4009.

[32] Zhu, Leize, et al. "Rheological properties of redox-responsive, associative ferrocene-modified branched poly (ethylene imine) and its modulation by β-cyclodextrin and hydrogen peroxide." *Soft Matter* 6.21 (2010): 5541-5546.

[33] Petersen, Robert J. "Composite reverse osmosis and nanofiltration membranes." *Journal of membrane science* 83.1 (1993): 81-150.

[34] Tang, Chuyang Y., Young-Nam Kwon, and James O. Leckie. "Effect of membrane chemistry and coating layer on physiochemical properties of thin film composite polyamide RO and NF membranes: II. Membrane physiochemical properties and their dependence on polyamide and coating layers." *Desalination* 242.1-3 (2009): 168-182.

[35] Briggs, David, and Graham Beamson. "XPS studies of the oxygen 1s and 2s levels in a wide range of functional polymers." *Analytical Chemistry* 65.11 (1993): 1517-1523.

[36] Vrijenhoek, Eric M., Seungkwan Hong, and Menachem Elimelech. "Influence of membrane surface properties on initial rate of colloidal fouling of reverse osmosis and nanofiltration membranes." *Journal of membrane science* 188.1 (2001): 115-128.

국문초록

본 연구에서는 역삼투 분리막에 전기장에 감응하는 페로센과 베타 사이클로덱스트린 복합체(ferrocene-cyclodextrin complex)가 도입된 가지구조형 폴리에틸렌이민(branched Polyethylenimine, b-PEI)을 화학적 결합을 이용해 개질하여, 전기장에 감응하는 분리막을 제조하였다. 이 분리막은 가지구조형 폴리에텔렌이민에 의한 높은 친수성으로 내파울링 성질을 가지며, 전기장에 의해 페로센이 산화되어 사이클로덱스트린이 파울런트들과 함께 떨어져 나가게 만들어 높은 회복 성질을 보였다. 먼저, 가지구조형 폴리에틸렌이민에 페로센의 양을 조절하여 합성하였다. 상용되는 역삼투 분리막은 EDC와 NHS를 이용하여 표면을 불안정한 상태로 만든 후, 합성된 고분자를 도입하였다. 다음으로 베타 사이클로덱스트린을 도입함으로써 전기장에 재생할 수 있는 오염 저감 분리막을 제조하였다. 가지구조형 폴리에틸렌이민과 페로센의 성공적인 합성은 푸리에 변환 적외선 분광광도계 (FT-IR)와 수소 핵자기 공명 분광 (^{1}H-NMR) 분석을 통해 확인하였으며, 동적 광산란 (DLS) 분석을 통해 페로센의 조성이 증가할수록 합성된 고분자의 크기가 증가하는 것을 확인하였다. 분리막 제조 후, 감쇠 전반사 적외선 분광광도계 (ATR-FT-IR)과 광전자 분광기 (XPS) 분석에 의해 베타 사이클로덱스트린의 성공적 도입과 페로센의 조성에 따른 합성된 고분자와 베타 사이클로덱스트린을 정성적, 정량적으로 확인 할 수 있었다. 주사전자현미경 (FE-SEM)과 원자간력현미경 (AFM) 관찰 결과 개질 후에도 분리막은 역삼투 분리막의 융선 골 구조를 유지하는 것을 관찰 하였고, 접촉각 측정을 통해 분리막의 친수성이 증가됨을 확인하였다. 전기장에 의한 재생 효과는 카본 판을 전극으로 써서 진행을 하였다. 사이클로덱스트린의 유무를 적외선 분광광도계, 광전자 분광기, 접촉각 측정을 통해 관찰 하였으며 성공적으로 사이클로덱스트린이 전기장에 의해 재생됨을 확인하였다. 성능 평가를 위해 수투과 테스트와 소금을 이용해 염 제거율 평가를 진행했으며, 개질 후에도 95% 이상의 높은 염 제거율을 가지는 것을 확인하였다. 합성된 고분자의 경우 페로센의 조성이 증가할수록 뭉치려는 성질에 의해 크기가 커지므로 높은 조성의 페로센으로 개질된 분리막의 경우 낮은 수투과도를 나타내었다. 따라서, 페로센의 양을 조절하여 상대적으로 높은 수투과도를 보인 분리막중 사이클로덱스트린의 도입양이 많은 조성의 분리막이 회복성능을 보기에 가장 적합하다고 판단하였다. 최종적으로, 오염에 대한 회복 성능과 내오염성을 확인하기

위하여 양이온 계면활성제를 사용하여 개질 전과 개질 후의 분리막에 투과평가를 3회에 걸쳐 진행한 후 전기장을 가했다. 그 결과 개질된 분리막은 일반 분리막에 의해 오염물질에 의한 수투과도의 감소 폭이 적었다. NaOCl을 이용하여 세척을 한 경우 44%의 높은 회복률을 보였지만 투과평가가 진행 될수록 효과가 작아지는 것을 확인 하였고 개질된 분리막의 경우 수투과도의 회복률이 77%로 크게 향상되었다. 오염된 분리막 표면은 전기장에 의한 사이클로덱스트린의 재생을 통해 복구될 수 있으며, 이는 막오염에 따라 감소했던 수투과도가 전기장을 주고 나서 86% 수준으로 매우 높게 복원되는 것을 통해 확인하였다. 이러한 전기장 감응성 재생가능한 분리막은 실제 역삼투 분리막 공정에서 세척 없이 간단한 전기장을 주어 재생시킴으로써 분리막의 장기간 사용에 도움이 될 것으로 기대된다.